

**SAFT- γ Force Field for the Simulation of Molecular Fluids:
8. Hetero-Group Coarse-Grained Models of Perfluoroalkylalkanes Assessed with
New Vapour-Liquid Interfacial Tension Data**

Pedro Morgado¹, Olga Lobanova², Miguel Almeida¹, Erich A. Müller², George Jackson²,
and Eduardo J. M. Filipe^{1*}

¹ Centro de Química Estrutural, Instituto Superior Técnico, Universidade de Lisboa, 1049-001
Lisboa, Portugal

² Department of Chemical Engineering, Centre for Process Systems Engineering, Imperial
College London, South Kensington Campus, London SW7 2AZ, UK

Abstract

The air-liquid interfacial behaviour of linear perfluoroalkylalkanes (PFAAs) is reported through a combined experimental and computer simulation study. The surface tensions of seven liquid PFAAs (perfluorobutylethane, F₄H₂; perfluorobutylpentane, F₄H₅; perfluorobutylhexane, F₄H₆; perfluorobutyloctane, F₄H₈; perfluorohexylethane, F₆H₂; perfluorohexylhexane, F₆H₆; and perfluorohexyloctane, F₆H₈) are experimentally determined over a wide temperature range (276 to 350 K). The corresponding surface thermodynamic properties and the critical temperatures of the studied compounds are estimated from the temperature dependence of the surface tension. Experimental density and vapour pressure data are employed to parameterize a generic heteronuclear coarse-grained intermolecular potential of the SAFT- γ family for PFAAs. The resulting force field is used in direct molecular dynamics simulations to predict with quantitative agreement the experimental tensions and to explore the conformations of the molecules in the interfacial region revealing a preferential alignment of the PFAA molecules towards the interface and an enrichment of the perfluoro-groups at the outer interface region.

* Corresponding author: efilipe@tecnico.ulisboa.pt

1. Introduction

Perfluoroalkylalkanes (PFAAs) are linear chain molecules formed from perfluorinated and hydrogenated alkyl segments chemically bonded together, with the general structure $F(CF_2)_i(CH_2)_jH$ (denoted as F_iH_j for conciseness). These substances can thus be envisaged as “chemical mixtures” of alkanes and perfluoroalkanes that, given their known mutual phobicity, would in most cases phase separate. The forced coexistence of an alkyl and a perfluoroalkyl segment in the same molecule give PFAAs a marked surfactant character¹, despite the absence of a polar head-group. Their amphiphilic nature is the result of a subtle balance of *weak* dispersion forces, which has earned these compounds the epithet of “primitive surfactants”². PFAA molecules are known to aggregate in solvents with a propensity for one of the blocks^{2,3}, and to form smectic (layered) liquid-crystalline phases^{4,5,6}, and molecular films displaying surprising patterns at the nanometric scale^{7,8}. Organization into layered structures in the solid state and surface freezing has also been described^{9,10,11,12,13,14}.

As a consequence PFAAs are expected to display interesting interfacial behaviour and an in-depth understanding is of clear importance for various applications. The surface tension, in particular, is a key property in the recently suggested use of PFAAs as liquid ventilation excipients for nebulized drug delivery¹⁵. Surface tensions have, however, only been experimentally determined for some relatively long PFAAs, which are solids at ambient temperature^{13,14,16}. A systematic study of this property as a function of the relative length of the hydrogenated and fluorinated segments is therefore very timely.

Comprehensive computational studies focusing on the interfacial properties of the PFAA molecules have been performed by Hariharan and Harris¹⁷ and by Pierce *et al.*¹⁸. A united-atom approach was used by Hariharan and Harris¹⁷ to examine the surfaces of *n*-decane, perfluoro-*n*-decane, F_5H_5 , and $F_{10}H_{10}$ in terms of surface tension, density profiles and molecular orientations; their study indicated that in PFAA molecules the perfluorinated segments tend to segregate to the surface and are preferentially oriented perpendicularly to the interface. With their model, however, one is unable to distinguish between the surface tension of alkanes and perfluoroalkanes. Pierce *et al.*¹⁸ used two different force fields to study the interfacial behavior of a number of PFAAs,

alkanes, and perfluoroalkanes: the optimized OPLS-AA model based on *ab initio* calculations by Pádua¹⁹; and the exponential-6 force field based on the *ab initio* model for perfluoroalkanes developed by Borodin *et al.*²⁰ The predicted surface tensions of PFAAs were sometimes lower than both the *n*-alkane and perfluoro-*n*-alkane with the same number of carbon atoms. Pierce *et al.*¹⁸ again found segregation of the fluorinated segments to the surface, with a normal orientation of the molecules relative to the interface. However, the simulated densities and surface tensions were essentially compared with experimental data for the *n*-alkanes. Only a single experimental density and surface tension at a given temperature were available for one perfluoro-*n*-alkane and one PFAA.

It becomes apparent from the foregoing discussion that given the scarcity of experimental data, the scope for the experimental validation of the simulation studies is very limited. The reliability and predictive value of molecular simulation is directly related to the underlying intermolecular potentials employed to describe the interactions between the chemical moieties making up the molecules. For the PFAA molecules, the interactions are generally based on force fields originally developed for pure *n*-alkanes and perfluoro-*n*-alkanes^{20,21,22,23,24,25,26}, together with the assumption that the parameters for the alkyl and perfluoroalkyl groups are transferable to the more complex di-block molecules. Deviations from ideal solution behavior are typically taken into account by adjusting cross interaction parameters to the properties of alkane – perfluoroalkane mixtures²⁷. This approach neglects the effect of the fluorinated chain section of the molecule on the adjacent alkyl moieties and the very asymmetric and polar nature of the connecting CF₂-CH₂ bond. The importance of this issue in developing force fields for mixed hydrocarbon – fluorinated molecules has been reviewed by Paulechka *et al.*²⁸ and by Lachet *et al.*²⁹.

Although atomistic simulations still remain a popular molecular modeling technique, coarse-grained (CG) models have received substantial attention within the molecular simulation community over the last two decades^{30,31}. The main advantage of a CG description is the increased computational efficiency, which enables access to large system sizes and slow processes that require long computational times. At the heart of a molecular simulation is the underlying force field, the accuracy of which determines

the adequacy of the simulation in describing the system of interest. A key issue in developing a CG force field is therefore the methodology employed to parameterize the intermolecular potentials. One can think of coarse graining as a way to “upscale” an atomistic or finer resolution model, reducing the number of degrees of freedom and effectively integrating out the molecular detail. Some of the common techniques of this so-called “bottom-up” approach include iterative Boltzmann inversion,³² force matching,³³ and inverse Monte Carlo.³⁴ A good overview of CG techniques is provided in the recent reviews by Noid³⁵ and Brini *et al.*³⁶

We employ a fundamentally different approach here, developing the force-field parameters by optimizing the description of target macroscopic thermophysical properties, in this instance the saturated liquid density and vapour pressure, for representative compounds with an analytical equation of state (EoS). The third-generation version of the statistical associating fluid theory (SAFT) based on the Mie intermolecular potential, SAFT- γ Mie EoS³⁷, is employed to parameterize the molecular force fields. The SAFT- γ Mie EoS is a group contribution reformulation^{38,39} of the SAFT-VR Mie⁴⁰ analytical free energy for associating chain molecules, and a successor of the original first-generation SAFT^{41,42} and the second-generation SAFT-VR^{43,44} EoSs. The SAFT- γ Mie EoS is used here to inform CG force-field parameters representing the interactions between the chemical groups characteristic of PFAA molecules that can then be used as input in direct molecular simulation. The SAFT- γ Mie methodology has already been applied to develop an efficient parameterization of CG force fields over a broad range of conditions for a variety of molecular fluids, including carbon dioxide^{45,46,47}, other greenhouse gases and refrigerants⁴⁸, aromatic compounds,⁴⁹ water and aqueous mixtures^{50,51,52,53}, *n*-alkanes^{48,54}, and amphiphilic systems comprising nonionic⁵⁵, light-switching⁵⁶, and super spreading surfactants⁵⁷. The procedure for the determination of the molecular parameters can be further simplified with a corresponding states treatment⁵⁸. For details of the SAFT- γ Mie methodology and specific examples of the capabilities of the CG force fields, the reader is referred to a recent review⁵⁹.

In addition to the higher resolution (atomistic and united-atom) force fields mentioned earlier, CG models have also been developed for *n*-alkanes^{60,61,62,63} and for perfluoro-*n*-alkanes^{64,65}; we are not, however, aware of an integrated CG model which can deal quantitatively with the subtleties of having the two chemical moieties fused on the PFAA molecule. For this purpose, the SAFT- γ Mie force fields developed in our current study are assessed by comparing the simulated and experimental surface tension data of PFAAs which are not used to parametrize the model; the comparison thus serves as a validation of the molecular models.

It is worth noting that various versions of the SAFT EoS have been applied to study the macroscopic phase behavior of systems involving *n*-alkanes and perfluoro-*n*-alkanes. For instance, the fluid-phase behavior of the binary alkane – perfluoroalkane mixtures has been investigated extensively with the SAFT-HS^{66,67}, SAFT-VR^{68,69}, soft-SAFT⁷⁰, PC-SAFT⁷¹, and hetero-SAFT VR⁷² EoSs. The properties of the PFAA molecules including the volumetric properties^{73,74}, vapour pressures⁷⁵, and solution behaviour of mixtures with *n*-alkanes and perfluoro-*n*-alkanes^{72,76,77} have also been examined with the hetero-SAFT VR EoS⁷⁸. These EoSs cannot, however, be used on their own to describe the interfacial tension of the systems unless they are incorporated in other approaches such as density functional^{79,80,81} or square gradient^{52,82,83} theories.

The surface tension of seven liquid PFAA molecules are measured experimentally over a wide temperature range (276 to 350 K). The new data fills an important gap in the available properties for this family of compounds and is used to complement and validate the modeling effort. The critical temperatures of the compounds are estimated from the temperature dependence of the surface tension. The results are interpreted by comparison with the corresponding properties for *n*-alkanes, perfluoro-*n*-alkanes, and their mixtures, though the analysis is hampered by the lack and inconsistency of existing data.

2. Experimental Details

Ultra-purified linear perfluorobutylpentane (F₄H₅), perfluorobutylhexane (F₄H₆), perfluorobutyloctane (F₄H₈), perfluorohexylhexane (F₆H₆), and perfluorohexyloctane

(F_6H_8) are obtained from Fluoron GMBH, with a reported purity of 100%; ^{19}F and 1H NMR spectra of these samples obtained with a Bruker Avance III 500MHz spectrometer indicate only very small unexpected peaks corresponding to relative integrated values smaller than 1%. Perfluorobutylethane (F_4H_2) (99%) and perfluorohexylethane (F_6H_2) (97%) are purchased from Apollo Scientific Ltd. Hexadecane (99%) and perfluorohexane (99%) are supplied by Sigma-Aldrich. All liquids are used as received, without any further purification.

The densities of perfluorobutylethane (F_4H_2) and perfluorohexylethane (F_6H_2) are measured at atmospheric pressure with an Anton Paar DMA5000 vibrating tube densimeter, according to the procedure described in previous work.⁷⁴

The surface tensions are determined using the pendant drop method. The drop images are produced using a CCD camera, mounted on an optical microscope, and recorded on a computer through an image acquisition board; the drops are illuminated from behind using a variable-intensity tungsten lamp and an optical diffuser. The analysis of the drop profiles is performed with the axisymmetric drop shape analysis (ADSA) method, developed by Hoorfar and Neumann⁸⁴. The image analysis software requires the acquisition of a photograph of a square grid etched on glass (supplied by Graticules Ltd.), to calibrate the pixel size and correct for eventual optical distortion.

The drops are formed inside an optically flat cell, which is itself inside an aluminium thermostatic cell with optical windows. A specially constructed stainless steel drop holder⁸⁵ (3 mm diameter) is used to suspend the drops, in order to obtain larger profiles and, hence, a lower experimental uncertainty. The thermostatic cell is kept at a constant temperature using a circulating bath. The temperature is measured as close as possible to the drop, using a calibrated platinum resistance thermometer mounted inside a thin-walled glass tube; the stability during the measurements is found to be better than 0.1 K.

During the measurements, liquid PFAA is kept inside a Hamilton glass and PTFE syringe, connected to the drop holder by a PTFE tube; an electronic syringe pump (New Era NE-300) is used to precisely control the size of the drops. For each data point at a single temperature, at least 50 independent images of at least 10 different drops are

collected, and the average value and standard deviation recorded. The liquid densities of the PFAAs, required for the calculation of the surface tension from the drop profiles, are determined in our current study or taken from previous work^{73,74}.

The apparatus and the measuring method are tested by determining the surface tension of *n*-hexadecane as a function of temperature, and also of perfluoro-*n*-hexane at a single temperature. This data is reported in Table 1. The tensions for *n*-hexadecane have the same temperature dependence and are *ca.* 0.3 mN m⁻¹ lower than the reference data reported by Jasper⁸⁶ and by Korosi and Kovats⁸⁷. The data point for perfluoro-*n*-hexane agrees, within the experimental uncertainty, with the values reported by Stiles and Cady⁸⁸, McLure *et al.*⁸⁹, and Nishikido *et al.*⁹⁰.

Table 1. Experimental surface tension γ of *n*-hexadecane and perfluoro-*n*-hexane

<i>n</i> -hexadecane		perfluoro- <i>n</i> -hexane	
<i>T</i> / K	γ / (mN m ⁻¹)	<i>T</i> / K	γ / (mN m ⁻¹)
299.9	26.57 ± 0.03	298.9	11.29 ± 0.09
314.1	25.39 ± 0.03		
329.1	24.05 ± 0.04		
344.3	22.78 ± 0.02		

3. Molecular Models and Simulation Details

3.1 Force Field

In our current study, we develop the SAFT- γ CG Mie force field for PFAA components, based on the Mie intermolecular potential to describe the interactions between the various chemical segments. The Mie potential is a generalized form of the Lennard-Jones potential and can be expressed as⁴⁰

$$u(r) = C\varepsilon \left[\left(\frac{\sigma}{r} \right)^{\lambda_r} - \left(\frac{\sigma}{r} \right)^{\lambda_a} \right], \quad (1)$$

where C guarantees that the minimum of the potential energy $u(r)$, as a function of the center-to-center distance r , corresponds to $-\varepsilon$. The value of σ characterizes the diameter of the segment. The exponents are used to describe the general shape and

range of the potential discerning between a repulsive and attractive contribution, respectively. In our work, the attractive exponent is fixed to the London value of $\lambda_a = 6$ and for conciseness we drop the subscript of the repulsive exponent, $\lambda_r = \lambda$. The pre-factor C then takes the value of

$$C = \left(\frac{\lambda}{\lambda - 6} \right) \left(\frac{\lambda}{6} \right)^{6(\lambda - 6)}. \quad (2)$$

For an abridged discussion on the history and development of commonly used pairwise intermolecular potential functions and how the Mie function relates to other models, the reader is referred to the introduction given in Reference [40].

The PFAA molecules are represented as chains of tangentially bonded coarse-grained Mie segments, described with a generic transferable parameter set based on a group contribution approach. The various CG sites are defined in Table 2, and the composition of specific groups employed to represent the different PFAA is illustrated in Figure 1. Molecular models developed allow one to represent all of the PFAA components studied experimentally in our current work (F_4H_2 , F_4H_5 , F_4H_6 , F_4H_8 , F_6H_2 , F_6H_6 and F_6H_8), and can also be used to describe molecules of a different chain length compatible with the chosen mapping.








3.2 SAFT- γ CG Mie Force Field

Both the SAFT- γ EoS and the CG force field used in the simulations are based on the same Mie intermolecular potential, and this close correspondence between the theory and simulations is exploited as a means of accurately determining the parameters of the intermolecular potential. More specifically, the parameters are estimated with the SAFT- γ Mie EoS³⁷ by optimizing the description of the experimental liquid densities and vapour pressures of the pure components and the liquid-liquid equilibria of the corresponding mixtures. We present only a concise summary of the model development.

The force-field parameters for the end CE (C_3H_7-) and middle CM ($-C_3H_6-$) CG groups of the alkyl chain are taken directly from the hetero-segmented models for n -alkanes,

developed in Reference [54]. The C4 (C₄H₉ –) CG group is parameterized from the vapour-liquid equilibria of *n*-octane, which is represented as two C4 CG groups. In the case of the perfluorinated alkanes (C₄F₁₀, C₆F₁₄, and C₈F₁₈), hetero-segmented models are developed, which consist of differentiated end FE (CF₃ –) and middle FM (– C₂F₄ –) perfluorinated alkyl CG groups.

Table 2. CG group name and atomistic description.

Name	All-atom	Colour scheme
FE	CF ₃ –	
FM	– C ₂ F ₄ –	
FH	– CF ₂ C ₂ H ₄ –	
FHE	– CF ₂ C ₂ H ₅	
CE	C ₃ H ₇ –	
CM	– C ₃ H ₆ –	
C4	C ₄ H ₉ –	

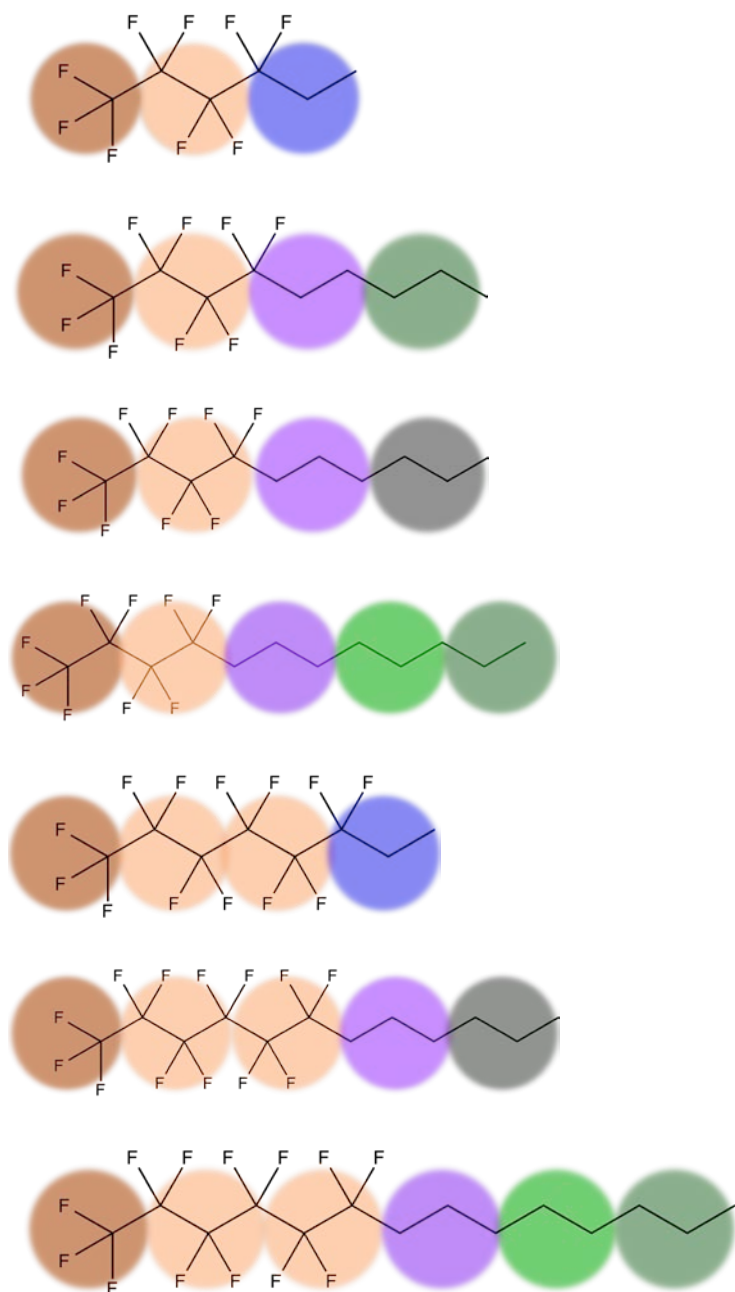


Figure 1. CG molecular models of linear perfluoroalkylalkanes $F(CF_2)_i(CH_2)_jH$ (denoted as F_iH_j), from top to bottom: F_4H_2 , F_4H_5 , F_4H_6 , F_4H_8 , F_6H_2 , F_6H_6 , and F_6H_8 . The color scheme is as indicated in Table 2.

The unlike interactions between different groups making up the perfluoroalkylalkane molecules are obtained by using simple combining rules⁴⁰. The unlike size parameter σ_{ij} is obtained from the classical Lorentz arithmetic combining rule:

$$\sigma_{ij} = \frac{\sigma_i + \sigma_j}{2}. \quad (3)$$

The unlike repulsive exponents are calculated using the following relationship:

$$\lambda_{ij} - 3 = \sqrt{(\lambda_i - 3)(\lambda_j - 3)}. \quad (4)$$

The unlike energy parameter ε_{ij} is obtained from a modified Berthelot-like geometric combining rule,

$$\varepsilon_{ij} = (1 - k_{ij}) \frac{\sqrt{\sigma_i^3 \sigma_j^3}}{\sigma_{ij}^3} \sqrt{\varepsilon_i \varepsilon_j}, \quad (5)$$

where k_{ij} is a binary adjustable parameter, which allows for an improved representation of the unlike attractions^{91,92}. In our current work, the k_{ij} parameter (or the ε_{ij} parameter) is adjusted either to the properties of the corresponding mixture or where appropriate to the pure component vapour-liquid equilibria; the latter highlights a key advantage of employing a hetero-segmented model within the SAFT- γ description.

The unlike interactions between FE – CE, FE – CM, FE – C4, FM – CE, FM – CM, FM – C4 pairs of groups are estimated from the experimental liquid-liquid phase-equilibrium data for the C₆F₁₄ + C₆H₁₄, C₈F₁₈ + C₆H₁₄, C₈F₁₈ + C₉H₂₀, and C₈F₁₈ + C₈H₁₈ binary mixtures^{67,70,93,94,95,96,97,98,99,100,101,102}. The connecting groups (FH and FHE), which bridge the alkyl and the perfluoroalkyl chains, are introduced to account for the presence of the dipole moment between the two chemical moieties in an effective manner; the FH and FHE groups are characterized by dispersion energies which differ markedly different from the values for the alkyl (CE, CM, C4) or perfluoroalkyl (FE, FM) groups. The like and unlike interactions of the FH and FHE groups with the FE, FM, CE, CM, and C4 groups are estimated with the SAFT- γ Mie EoS³⁷ from the experimental liquid densities and vapour pressures of the F₄H₂, F₄H₅, F₄H₆, F₄H₈, F₆H₂, F₆H₆, and F₆H₈

pure components^{73,74,75}. The final SAFT- γ Mie parameter set for the CG groups characterizing the PFAA molecules is summarized in **Table 3**.

Table 3. Intermolecular and intramolecular potential parameters of the SAFT- γ CG Mie force field for the CG perfluoroalkylalkanes groups (defined as in Table 2): σ is the size parameter; ε is the depth of the potential; λ is the repulsive exponent (the attractive exponent is set to the London value of 6 in all cases). The unlike parameters σ_{ij} and λ_{ij} between groups of different type are calculated directly from the combining given in Eqs. 3 and 4, and are included in the table for completeness. The intramolecular interactions are represented with harmonic potentials characterized by the bond stretching k_{bond} and the bending k_{angle} spring constants, with the distance r_0 and the angle θ_0 at the potential minimum. The parameters for the CE and CM CG groups of the pure-component n -alkanes are those developed in Reference [54].

Intermolecular Parameters				
Group 1	Group 2	$\sigma / \text{\AA}$	$(\varepsilon / k_B) / \text{K}$	λ
FE	FE	3.818	200.79	16.24
FM	FM	4.020	226.52	11.91
FH	FH	4.540	336.37	17.69
FHE	FHE	4.764	336.37	17.69
CE	CE	4.500	358.37	15.95
CM	CM	4.180	377.14	16.43
C4	C4	5.001	473.62	24.00
FE	FM	3.919	218.12	13.86
FE	FH	4.179	308.36	16.95
FE	FHE	4.291	308.36	16.95
FE	CE	4.159	245.63	16.09
FE	CM	3.999	253.76	16.33
FE	C4	4.410	283.59	19.67
FM	FH	4.280	269.67	14.44
FM	FHE	4.392	269.67	14.44
FM	CE	4.260	262.30	13.74
FM	CM	4.100	270.21	13.94
FM	C4	4.511	304.05	16.68
FH	CE	4.520	361.88	16.79
FH	CM	4.771	377.29	20.57
FH	C4	4.360	328.83	17.05
CE	CM	4.340	345.72	16.19
Intramolecular Parameters				
Between Groups	$k_{bond} / (\text{kJ mol}^{-1} \text{\AA}^{-2})$	$r_0 / \text{\AA}$	$k_{angle} / (\text{kJ mol}^{-1} \text{rad}^{-2})$	θ_0 / deg
FE, FM, FH, FHE	61.30	σ	17.66	180.0
CE, CM, C4	61.30	σ	17.66	159.9

In addition to the intermolecular interactions, obtained with the SAFT- γ Mie EoS, intramolecular interactions are incorporated into the models in order to account for the chain rigidity. The intramolecular interactions are described with harmonic potentials that include bond stretching and bond angle bending,

$$u_{\text{intra}} = \sum_{\text{bond}} \frac{1}{2} k_{\text{bond}} (r - r_0)^2 + \sum_{\text{angle}} \frac{1}{2} k_{\text{angle}} (\theta - \theta_0)^2, \quad (6)$$

where k_{bond} and k_{angle} are the corresponding spring constants, with r_0 and θ_0 as the distance and angle at the potential minimum. The beads are kept together with a rather stiff spring which keeps the beads at a distance close to σ . The backbone of the perfluorinated chain of the molecular is kept essentially linear by setting $\theta_0 = 180^\circ$ (owing to the extra rigidity of the bulky fluorinated groups), while the backbone of the alkyl chain is characterized by angle of $\theta_0 = 159.9^\circ$ subtended by the groups. The intramolecular parameters are taken directly from those developed for CG alkane chains in Reference [54] without modification, as summarized in Table 3; the values characterizing the temperature of 400 K are preferable here owing to the temperature range of interest in our current work.

3.3 Molecular Simulation Details

The thermodynamic and interfacial properties of PFAA molecules, represented with the SAFT- γ CG Mie models described in the previous section, can now be determined from the direct molecular dynamics (MD) simulation¹⁰³ in the canonical ensemble, corresponding to a constant number of particles N , volume V , and temperature T . The overall density of the system is chosen such that it lies inside the coexistence envelope according to the simulation procedure outlined in Reference [104].

A system of $N = 3000$ PFAA molecules is simulated in an orthorhombic simulation box with the usual periodic boundary conditions, where the box length L_z in the z direction is chosen such that it is three times longer than that in the x and y directions. At the start of the simulation a cubic box filled with molecules at the desired liquid density is placed between two empty cubic boxes corresponding to vapour; the dimension of the system is typically $\sim 30 \times 30 \times 90$ segment diameters, the actual values dependent on the system density and chemical structure of the molecules. In this configuration, a liquid slab develops with two planar interfaces in contact with low-density vapour. The simulations are carried out using the Gromacs package (version 4.5.5)¹⁰⁵ and the equations of motion are solved using the leap-frog algorithm with a time step of 10 fs. The system temperature is maintained constant using the Nosé-Hoover thermostat^{106,107} with a coupling constant of 1.0 ps. The first 700,000 time steps are discarded and the equilibrium properties are then sampled for an additional 700,000 time steps to obtain time averages of the properties of interest. The cutoff radius for all group interactions is fixed to 30 Å; this value has been shown to provide reliable estimated of the thermodynamic properties (and the interfacial tension in particular) for Mie potentials of relatively long range^{50,53}.

The densities of the coexisting vapour and liquid phases are determined from the density profiles at the corresponding temperature. The vapour-liquid interfacial tension γ is calculated by means of a mechanical route^{108,109}, which requires the evaluation of forces in order to obtain the average Cartesian components $P_{\alpha\alpha}$ of the pressure tensor:

$$\gamma = \frac{1}{2} \int_0^{L_z} \left\{ P_{zz}(z) - \frac{1}{2} (P_{xx}(z) + P_{yy}(z)) \right\} dz. \quad (7)$$

4. Results and Discussion

4.1 Experimental Surface Tension of Perfluoroalkylalkanes

The liquid densities of F_4H_2 and F_6H_2 are measured at a series of temperatures between 278.15 K and 353.15 K. The densities are described with a polynomial of the form:

$$\frac{\rho}{\text{g cm}^{-3}} = C_0 + C_1 \left(\frac{T/\text{K}}{100}\right) + C_2 \left(\frac{T/\text{K}}{100}\right)^2 + C_3 \left(\frac{T/\text{K}}{100}\right)^3, \quad (8)$$

where ρ is the mass density, and C_i are adjustable coefficients. This relation provides a representation of the experimental values to within the experimental reproducibility. The corresponding values of the coefficients for the two PFAAs are shown in Table 4. The full set of experimental densities can be found as Supplementary Information.

Table 4. Coefficients of the polynomial (Eq. 8) to represent the liquid densities of the linear perfluoroalkylalkanes F_4H_2 and F_6H_2 over the range 278.15 to 353.15 K.

	C_0	C_1	C_2	C_3
F_4H_2	2.209116	-0.423535	0.0914281	-0.0129824
F_6H_2	2.278418	0.353018	0.0624866	-0.00857264

The vapour-liquid surface tensions of the PFAA molecules studied in our current work are recorded in Table 5, along with the respective standard deviations, and plotted in Figure 2. As expected, the surface tensions of all PFAAs decrease linearly over the temperature range of the measurements. It is also seen that, if the length of the perfluorinated chain segment is kept constant, the surface tension increases on increasing the length of the adjacent hydrogenated segment. On the other hand, the effect that changing the length of the fluorinated chain has on the surface tension of a given PFAA molecule depends on the length of the hydrogenated chain attached to it; for example, there is a significant increase in the value of the surface tension from F_4H_2 to F_6H_2 , but only a small increase from F_4H_6 to F_6H_6 , and almost no difference between

F₄H₈ and F₆H₈. This suggests that, beyond a given chain length, it is the length of the hydrogenated alkyl segment that dominates the value of the surface tension.

Table 5. Experimental vapour-liquid surface tension γ of the linear perfluoroalkylalkanes F_iH_j.

F ₄ H ₂		F ₄ H ₅		F ₄ H ₆	
T / K	$\gamma / (\text{mN m}^{-1})$	T / K	$\gamma / (\text{mN m}^{-1})$	T / K	$\gamma / (\text{mN m}^{-1})$
282.6	14.98 ± 0.07	277.1	18.69 ± 0.02	277.4	19.51 ± 0.02
285.9	14.66 ± 0.05	283.2	18.10 ± 0.02	282.1	19.04 ± 0.02
289.5	14.34 ± 0.06	288.5	17.47 ± 0.02	286.5	18.62 ± 0.02
292.9	14.05 ± 0.07	294.3	16.99 ± 0.01	293.1	17.96 ± 0.02
296.3	13.87 ± 0.05	300.7	16.46 ± 0.02	300.8	17.31 ± 0.03
301.0	13.36 ± 0.05	306.5	15.93 ± 0.02	307.7	16.62 ± 0.03
303.4	13.24 ± 0.04	314.7	15.22 ± 0.02	315.5	15.96 ± 0.03
		321.1	14.62 ± 0.03	322.3	15.37 ± 0.03
		328.2	14.00 ± 0.02	327.2	14.95 ± 0.02
		335.4	13.45 ± 0.02	334.8	14.31 ± 0.02
		343.0	12.85 ± 0.02	342.8	13.63 ± 0.03
		350.2	12.26 ± 0.02	349.1	13.14 ± 0.03

F ₄ H ₈		F ₆ H ₂		F ₆ H ₆	
T / K	$\gamma / (\text{mN m}^{-1})$	T / K	$\gamma / (\text{mN m}^{-1})$	T / K	$\gamma / (\text{mN m}^{-1})$
279.8	20.88 ± 0.03	282.7	16.51 ± 0.05	276.3	19.81 ± 0.02
285.8	20.26 ± 0.03	290.2	15.88 ± 0.04	282.8	19.25 ± 0.02
292.6	19.58 ± 0.02	296.0	15.48 ± 0.03	290.6	18.62 ± 0.01
296.5	19.23 ± 0.02	301.7	14.87 ± 0.06	299.2	17.81 ± 0.02
303.7	18.54 ± 0.02	309.8	14.19 ± 0.07	305.6	17.26 ± 0.02
310.2	18.05 ± 0.02	317.9	13.52 ± 0.04	313.4	16.65 ± 0.02
315.5	17.48 ± 0.03	322.0	13.19 ± 0.03	320.3	16.05 ± 0.01
320.5	17.08 ± 0.03			328.1	15.41 ± 0.01
329.9	16.31 ± 0.02			334.7	14.86 ± 0.02
337.8	15.66 ± 0.02			342.2	14.28 ± 0.02
347.6	14.84 ± 0.02			350.2	13.69 ± 0.02

F ₆ H ₈	
T / K	$\gamma / (\text{mN m}^{-1})$
277.6	20.73 ± 0.02
283.1	20.30 ± 0.02
289.2	19.69 ± 0.02
296.9	19.20 ± 0.03
301.1	18.90 ± 0.02
310.0	18.02 ± 0.02
314.3	17.74 ± 0.03
324.2	16.93 ± 0.03
334.7	16.07 ± 0.02
340.1	15.67 ± 0.02
349.9	14.86 ± 0.04

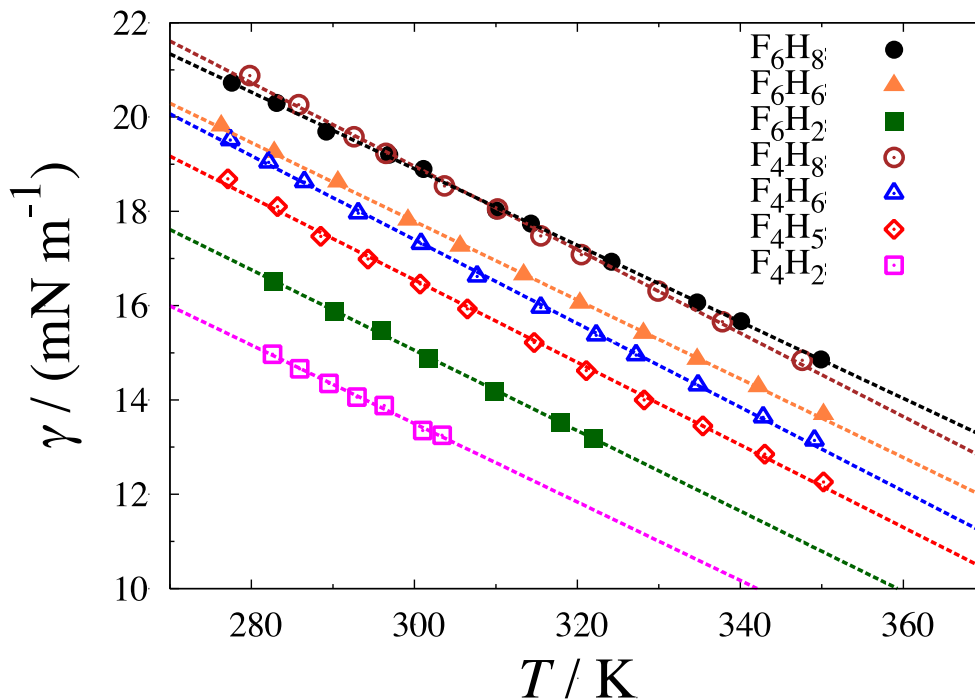


Figure 2. Experimental vapour-liquid surface tension γ of linear perfluoroalkylalkanes F_iH_j as a function of temperature T : \square , F_4H_2 ; \diamond , F_4H_5 ; Δ , F_4H_6 ; \circ , F_4H_8 ; \blacksquare , F_6H_2 ; \blacktriangle , F_6H_6 ; \bullet , F_6H_8 . The lines are least-square linear correlations of the data.

The measurements of the surface tension as a function of temperature can be used to provide a fairly accurate estimate of the critical temperature T_c using the empirical relations of Eötvös¹¹⁰ Eq. (9) and Guggenheim¹¹¹ Eq. (10):

$$\gamma V_m^{2/3} = A + BT; T_c = -A/B \quad (9)$$

$$\gamma = \gamma_0(1 - T/T_c)^{11/9} \quad (10)$$

where V_m is the orthobaric molar volume of the liquid, and A , B , and γ_0 are adjustable constants. Both relations are based on corresponding states correlations and reflect the vanishing surface tension at the critical point. It has been proposed that the agreement between estimates of the critical temperature following these two routes provides a good indication of the quality of the predictions¹¹².

The estimated critical temperatures of PFAA are presented in Table 6 and plotted in Figure 3 as a function of the overall chain length, along with the corresponding values for n -alkanes and perfluoro- n -alkanes. The predictions obtained from both relations

are in very good mutual agreement, differing by less than 1.5% in all cases. It can be seen from Figure 3 that the estimated critical temperatures of the PFAAs vary less with chain length than for either the *n*-alkanes¹¹³ or the perfluoro-*n*-alkanes¹¹⁴; the critical temperature of F₄H₂ is quite close to that of *n*-hexane, while T_c for F₄H₆ is already lower than that of *n*-decane and perfluoro-*n*-decane. This behavior is consistent with the vapour pressure data of PFAAs presented in previous work⁷⁵: shorter PFAA molecules are more cohesive than the corresponding *n*-alkanes and perfluoro-*n*-alkanes presumably because interactions between the permanent dipoles of the PFAAs are dominant. However, as the total chain length is increased, this effect becomes progressively less important and the weak interactions between the unlike segments starts to dominate the behavior, reducing the extent of cohesion in the liquid.

Table 6. Estimated critical temperatures T_c of the linear perfluoroalkylalkanes F_iH_j.

	T_c (Eötvos) / K	T_c (Guggenheim) / K
F ₄ H ₂	498.2	499.8
F ₄ H ₅	521.2	527.5
F ₄ H ₆	528.4	535.7
F ₄ H ₈	551.0	558.4
F ₆ H ₂	508.9	515.0
F ₆ H ₆	550.4	557.0
F ₆ H ₈	575.7	581.2

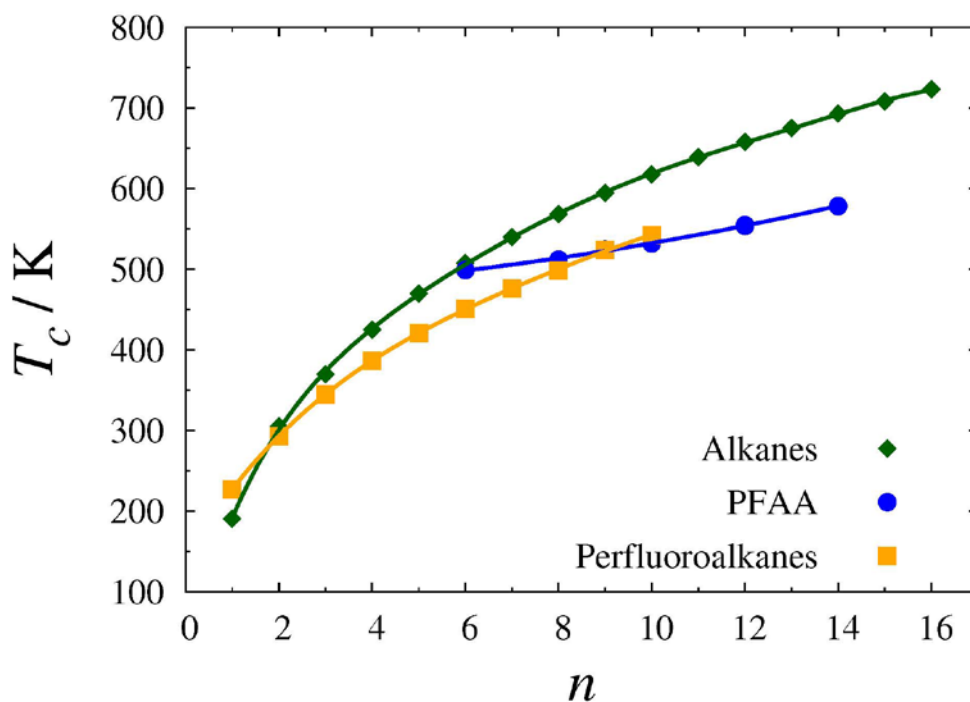


Figure 3. Critical temperatures T_c of linear alkanes¹¹³, perfluoroalkanes¹¹⁴, and perfluoroalkylalkanes (PFAA) as a function of the overall chain length n of the molecules.

It is instructive to compare the surface tensions with those of linear alkanes and perfluoroalkanes of similar chain length. This can be done by plotting the surface tension in terms of the reduced temperature $T_r = T/T_c$ (calculated using the average of the estimates for T_c from the Eötvs and the Guggenheim relations) as shown in Figure 4. When the surface tension is represented in terms of the reduced temperature, the experimental values for the n -alkanes⁸⁶ and perfluoro- n -alkanes^{115,116} are seen to follow essentially the same trend line for each chemical family. For the linear PFAA molecules with shorter alkyl chain segments (F_4H_2 and F_6H_2) the surface tensions are close to the values for the perfluoro- n -alkanes, while for the molecules with the highest degree of hydrogenation (F_4H_6 and F_4H_8) the values approach those for the n -alkanes. The remaining compounds fall essentially on the

same line, roughly equidistant from the values for the *n*-alkanes and perfluoro-*n*-alkanes.

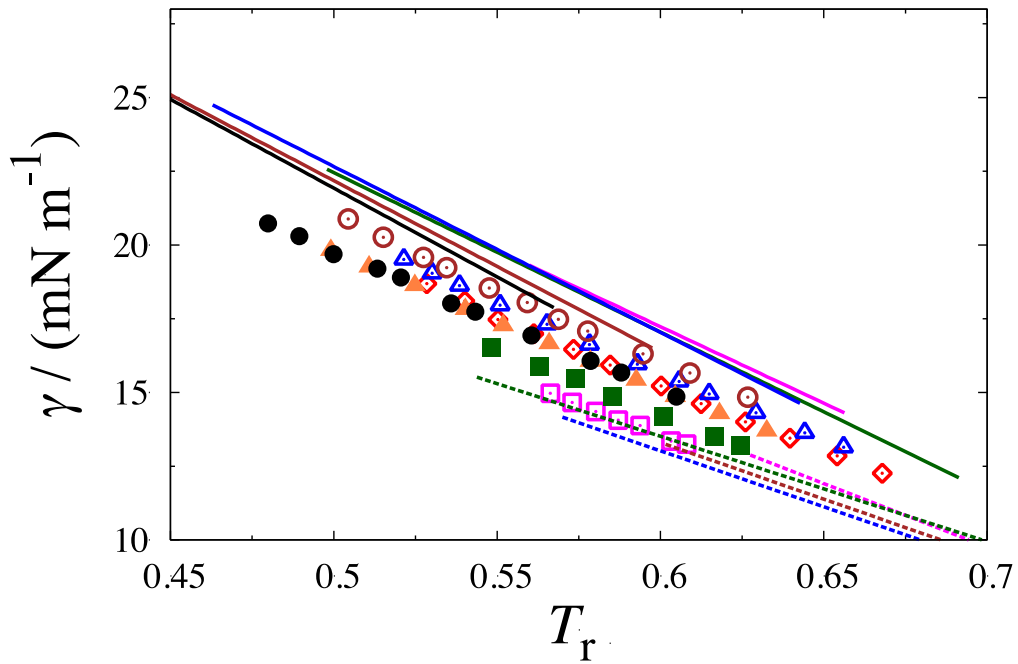


Figure 4. Surface tension γ of the linear perfluoroalkylalkanes (symbols as in Figure 2), the even numbered *n*-alkanes from C₆ to C₁₄ (continuous lines), and the even numbered perfluoro-*n*-alkanes from C₆ to C₁₂ (dashed lines), as a function of the reduced temperature T_r . The values for the *n*-alkanes are taken from the work of Jasper⁸⁶, and for the C₈ to C₁₂ perfluoro-*n*-alkanes from the work of Haszeldine and Smith¹¹⁵; the line for perfluoro-*n*-hexane is a linear regression of the data in References [88, 89, 90,116].

The surface tension can be identified with the surface Gibbs energy, at constant temperature and pressure¹¹⁷. The surface enthalpy H^γ and entropy S^γ can therefore be determined from the temperature dependence of the surface tension, assuming that both quantities are constant within the temperature range that is considered:

$$S^\gamma = -\left(\frac{\partial\gamma}{\partial T}\right) \quad (11)$$

$$H^\gamma = \gamma - T\left(\frac{\partial\gamma}{\partial T}\right) \quad (12)$$

The calculated surface thermodynamic functions for the studied PFAAs (cf. Table 7) are shown in Figure 5 together with those for the *n*-alkanes and perfluoro-*n*-alkanes (there are two PFAAs with the same overall chain length ($n = 12$), namely F6H6 and F4H8).

As can be seen, the surface enthalpy of the *n*-alkanes increases slowly with chain length suggesting the presence of stronger interactions as the molecules become longer. Perfluoro-*n*-alkanes display lower value of H^γ , revealing weaker cohesive interactions at the surface, in parallel with what is found in the bulk liquid. The trend for the perfluoro-*n*-alkanes is, however, not as clear, due to the large dispersion of the data. The linear PFAA molecules are characterized by surface enthalpies which are intermediate between the values of the corresponding *n*-alkanes and perfluoro-*n*-alkanes. The trend with the increasing length of each chain segment is consistent with the behavior of the *n*-alkanes and perfluoro-*n*-alkanes: H^γ increases with the number of carbon atoms in the hydrogenated chain segment when the fluorinated chain segment is kept constant, and, with the exception of the ethyl (-H₂) compounds, the opposite is seen when the number of fluorinated groups is increased.

By contrast, the surface entropy decreases with chain length for the *n*-alkanes; a similar behavior is seen for the perfluoro-*n*-alkanes, despite the considerable dispersion of the data. This suggests a progressive structuring of the surface as the chain length increases, for both families. The lower values of S^γ for the perfluoro-*n*-alkanes, especially for the longer molecules, suggests a higher degree of organization at the surface, probably due to their lower conformational freedom.

The PFAA molecules display intermediate values of S^γ , although the absolute values are now closer to those of the corresponding *n*-alkanes; this is probably due to the asymmetry of the PFAA associated with the presence of two types of segment, which increases the entropy. The PFAA molecules with longer perfluorinated chain segments (such as F₆) exhibit lower surface entropies than those with shorter segments (such as F₄), suggesting a higher degree of organization induced in the former. In the case of PFAAs with a constant perfluorinated chain length, S^γ remains essentially constant for the F₄H_j series and decreases slightly for the F₆H_j series. The ethyl substituted compound F₄H₂ appears to be an exception in the trend, probably due to the small

length of its segments. The dipolar character of this smaller molecule clearly dominates its amphiphilic characteristics.

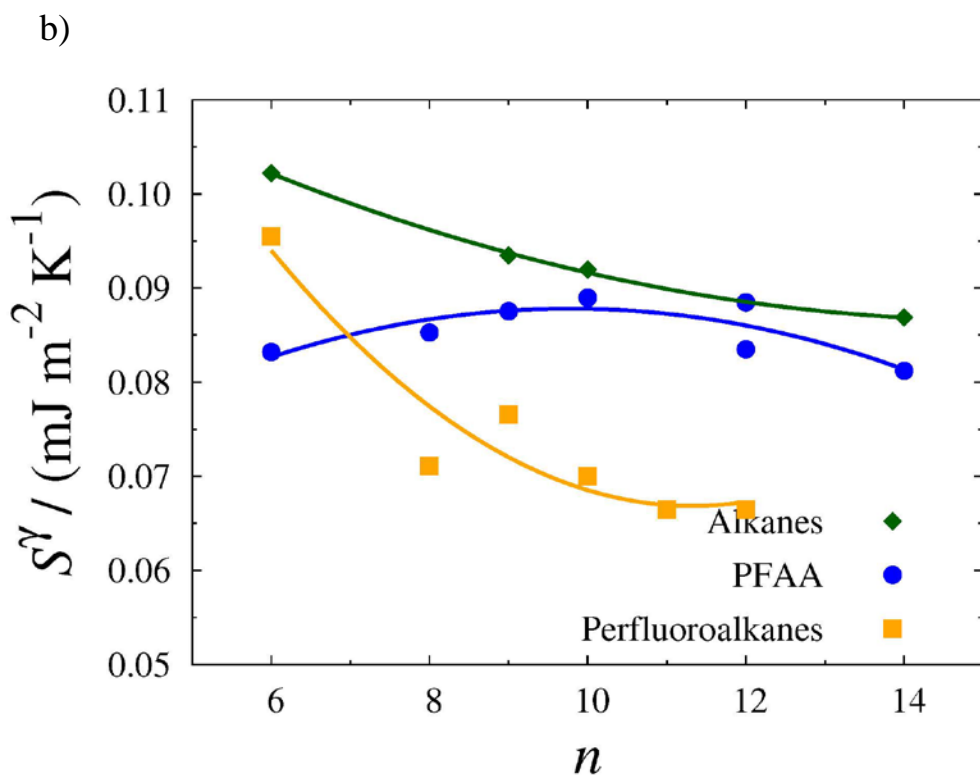
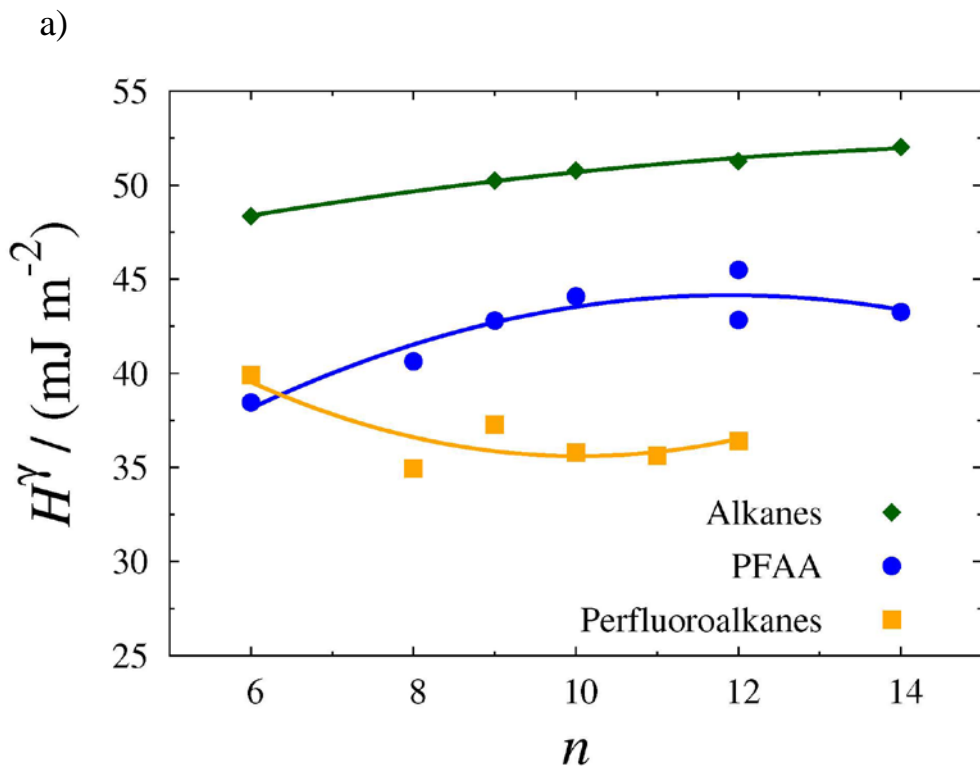


Figure 5. a) Surface enthalpy H^γ and b) surface entropy S^γ for the linear alkanes, perfluoroalkanes, and perfluoroalkylalkanes as a function of the total chain length n . The values for the n -alkanes and perfluoro- n -alkanes are determined from the surface tension correlations shown in Figure 4. The curves are polynomial fits, intended as a guide for the eye.

Table 7. Surface entropy S^γ and enthalpy H^γ for the linear perfluoroalkylalkanes F_iH_j .

	$S^\gamma / (\text{mJ m}^{-2} \text{K}^{-1})$	$H^\gamma / (\text{mJ m}^{-2})$
F_4H_2	0.083 ± 0.003	38.5 ± 0.8
F_4H_5	0.088 ± 0.001	42.8 ± 0.3
F_4H_6	0.089 ± 0.008	44.1 ± 0.3
F_4H_8	0.088 ± 0.001	45.5 ± 0.4
F_6H_2	0.085 ± 0.001	40.6 ± 0.4
F_6H_6	0.084 ± 0.006	42.8 ± 0.2
F_6H_8	0.081 ± 0.007	43.3 ± 0.2

Mixing hydrogenated and perfluorinated liquids are processes that involve large energetic and volumetric effects. Excess enthalpies higher than 1 kJ mol^{-1} and excess volumes above $5 \text{ cm}^3 \text{ mol}^{-1}$ are not uncommon. Large effects can therefore also be expected when hydrogenated and perfluorinated chains coexist at interfaces and a rationalization of the surface behavior of PFAA molecules should take this factor into account.

While it would be sensible to attempt to interpret the surface tension of PFAAs by comparison with the surface tension of an “equivalent” (n -alkane + perfluoro- n -alkane) mixture, at “equivalent” conditions, the analysis is not straightforward. As an example, the measured surface tension of F_6H_6 could be compared with the surface tension of an equimolar mixture of n -dodecane and perfluoro- n -dodecane, at similar experimental conditions. In practice, perfluoro- n -dodecane is solid over the relevant temperature range and there are no surface tension data available for this mixture. Most of the experimental data on mixtures of alkanes and perfluoroalkanes has been obtained in the group of McLure^{116,118}. Handa and Mukerjee¹¹⁹ have also studied a couple of binary mixtures. Several mixtures of alkanes ($C_5 - C_8$) and perfluoroalkanes ($C_6 - C_8$) have been examined at one or two temperatures, as well as a small number of mixtures involving other types of substances (alkylated polysiloxanes and perfluorotributylamine). McLure and co-workers^{120,121} have performed neutron

reflection experiments on the *n*-hexane + perfluoro-*n*-hexane mixture, supporting the assumption that a monolayer of the fluorinated component forms at the vapour-liquid interface for a range of temperatures both above and below the upper critical solution temperature (UCST). In all cases, the composition dependence of the surface tension exhibits large negative deviations from linear behavior (reflecting the preferential adsorption of the less dense perfluoroalkane). Sometimes minima in the surface tension are observed, a phenomenon referred to as *aneotropy*. Often the surface tension isotherm presents a horizontal inflection, which according to theoretical predictions reflects the proximity of an UCST¹²².

In spite of the scarcity of data, the conclusion that emerges from the aforementioned studies is that the coexistence of hydrogenated and perfluorinated chains at the interface can lead to lower surface tensions, in addition to the effect resulting from preferential adsorption of the fluorinated component. In the case of PFAA molecules the challenge is to assess the contribution to the surface tension (and hence the surface energy and orientation/organization) of bonding together the antagonistic segments. The contribution of the interaction between the dipole moment generated at this junction, not present in the parent molecules, should not be ignored.

Since a direct comparison of the surface tensions of PFAAs with those of the equivalent mixtures of alkanes and perfluoroalkanes is difficult, we adopt an alternative strategy of relating the surface tension to the molecular structure using the parachor $|P|$. This empirical quantity can be used to relate the vapour-liquid surface tension to the difference in the molar densities of the bulk coexisting liquid and vapour phases according to¹²³

$$\gamma^{1/4} = |P|(\rho_l - \rho_v) \quad (13)$$

The advantage of the approach relies on the fact that the parachor can be related to molecular functionality in an additive manner, following a group contribution approach^{124,125,126}. The contributions attributed to atoms or groups of atoms are taken to be constant, with small corrections to allow for structural features such as

branching or ring formation. For example, the atomic parachor of carbon $|P|(C) = 9.0$ and hydrogen $|P|(H) = 15.5$ for the n -alkanes are found to be essentially independent of the alkane and temperature¹²⁶.

Sakka and Ogata¹²⁷ examined the parachor of fluorine atoms in fluorinated alkanes and proposed a value for perfluoro- n -alkanes, $|P|(F) = 22.5$, which is much lower than that found for substituted alkanes with just one or two fluorine atoms, $|P|(F) = 26.1$. Their value was calculated using a very small set of the available data for perfluoro- n -alkanes. In our current work, we calculate the fluorine parachor contributions $|P|(F)$ as a function of temperature using a much larger pool of literature data^{88,89,90,116,128,129,130,131}, which includes that used by Sakka and Ogata. The molar densities used in the calculations are, whenever possible, those reported by the original authors. As can be seen from Figure 6, the fluorine parachor for perfluoro- n -alkanes is not constant, and ranges from ~ 21.5 to 23.5 , depending on the substance and temperature.

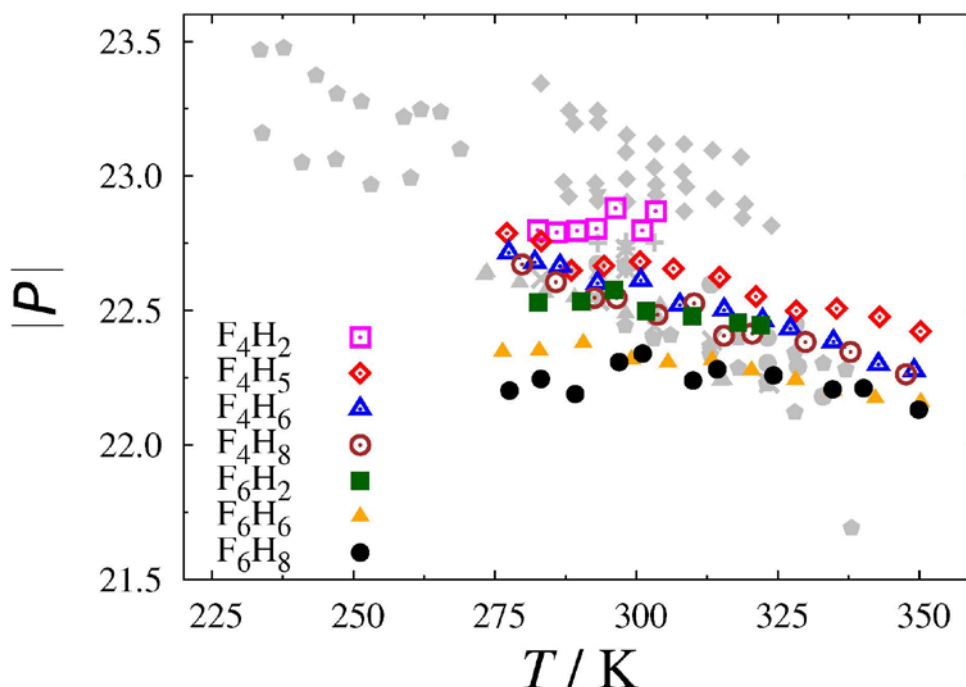


Figure 6. The temperature dependence of the fluorine atomic parachor $|P|(F)$ for linear perfluoroalkylalkanes F_iH_j calculated from the surface tensions measured in our

current work and for perfluoro-*n*-alkanes calculated from literature surface tension data: ×, Stiles and Cady⁸⁸; ◆, McLure *et al.*⁸⁹; *, Nishikido *et al.*⁹⁰; ●, McLure *et al.*¹¹⁶; ◆, Freire *et al.*¹²⁸; ▲, Rohrback and Cady¹²⁹; ▼, Fowler *et al.*¹³⁰; and +, Oliver *et al.*¹³¹.

We also calculate fluorine parachors for the PFAA molecules, and include them in Figure 6. As can be seen, the values for the PFAAs fall over a lower range of values than for the perfluoro-*n*-alkanes, and a closer inspection reveals that the fluorine parachors for the two PFAAs with longer fluorinated chains appear to be below the parachors for the perfluoro-*n*-alkanes, especially at the lower temperatures. This may indicate that PFAAs have slightly lower surface tensions than would be expected for their respective proportion of fluorinated and hydrogenated chains. At least part of this effect can be attributed to the coexistence of hydrogenated and perfluorinated chains at the interface that is not taken into account in the analysis.

4.2 Assessment of the SAFT- γ CG Mie Force Field for Perfluoroalkylalkanes

The temperature dependence of the saturated liquid density and the vapour pressure of the PFAA molecules is illustrated in Figures 7 and 8, respectively, for F_4H_2 , F_4H_5 , F_4H_6 , F_4H_8 , F_6H_2 , F_6H_6 , and F_6H_8 . The SAFT- γ Mie EoS³⁷ is seen to reproduce the available experimental data with high accuracy for the corresponding temperature range. The intermolecular parameters characterizing the CG beads estimated with the EoS (cf. Table 3) are subsequently used as force fields in the MD simulation. At the heart of the parametrization of the force field is the excellent agreement between the experimental data, the theoretical description with the SAFT- γ Mie EoS, and the corresponding molecular simulation data of the SAFT- γ Mie CG model. The vapour pressures of PFAAs are quite low, particularly for long chains and at low temperatures, and hence are difficult to obtain accurately from the simulations.

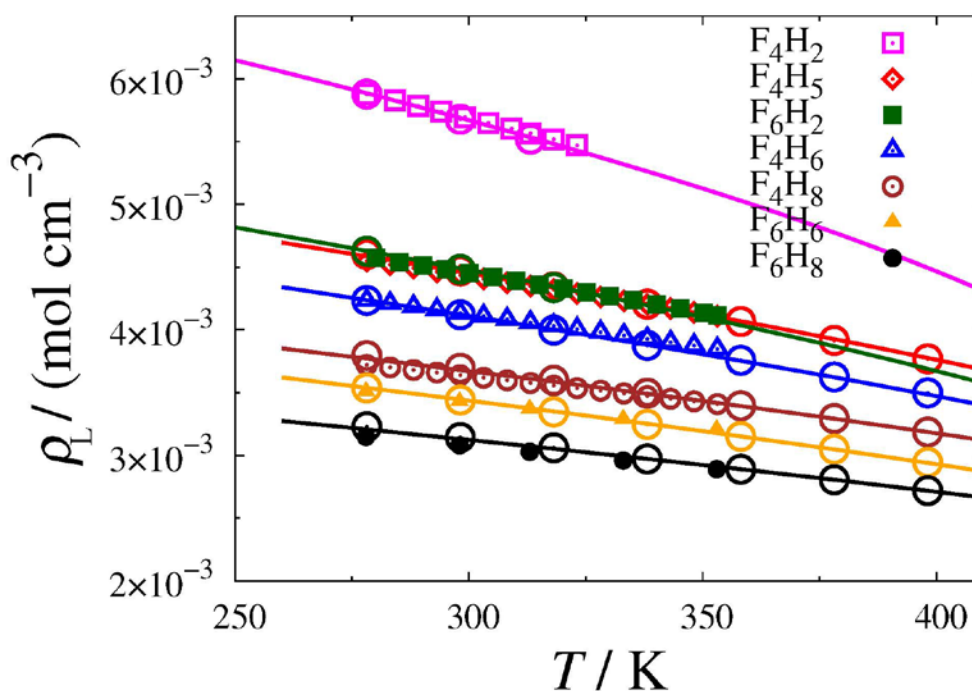


Figure 7. The temperature dependence of the saturated liquid density ρ_L for linear perfluoroalkylalkanes F_iH_j . The symbols represent the experimental data^{73,74}, the continuous curves correspond to the calculations with the SAFT- γ Mie EoS³⁷, and the large open circles denote the description obtained with the SAFT- γ Mie CG force field by molecular dynamics simulation using the same parameter set (cf. Table 3).

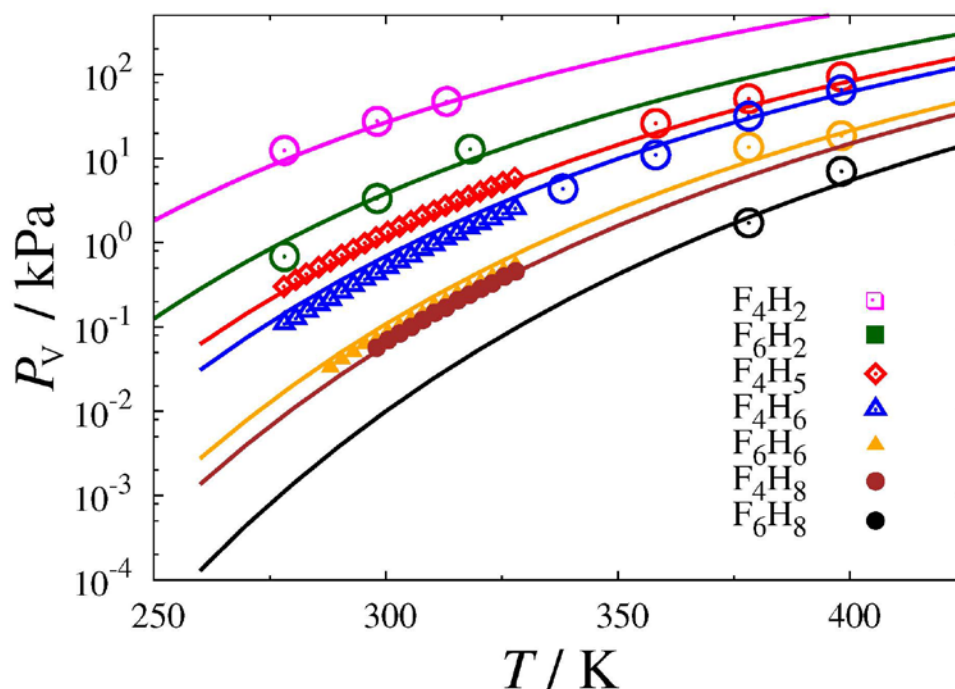


Figure 8. The temperature dependence of the vapour pressure P_v for linear perfluoroalkylalkanes F_iH_j . The symbols represent the experimental data⁷⁵, the continuous curves correspond to the calculations with the SAFT- γ Mie EoS³⁷, and the large open circles denote the description obtained with the SAFT- γ Mie CG force field by molecular dynamics simulation using the same parameter set (cf. Table 3).

The temperature dependence of the interfacial tension, illustrated in Figure 9, are true predictions with the SAFT- γ CG Mie force field, as the interfacial properties are not used as target properties in the estimation of the parameters of the model. The experimental data correspond to the air-fluid surface tensions, while the simulations are performed considering the vapour-liquid interface. The extremely low vapour pressures of the PFFAs and the small effect that pressure has on the interfacial tension make the distinction insignificant. Given that no interfacial tension data are used in the parametrization, the agreement between the simulated values and experiment is very encouraging. Experimentally observed trends, such as the marked increase in the interfacial tension relative to the values for the perfluoro-*n*-alkanes when an alkyl chain is introduced as compared to the small increase relative to the *n*-alkanes found on introducing a perfluoroalkyl chain, are well reproduced by the models.

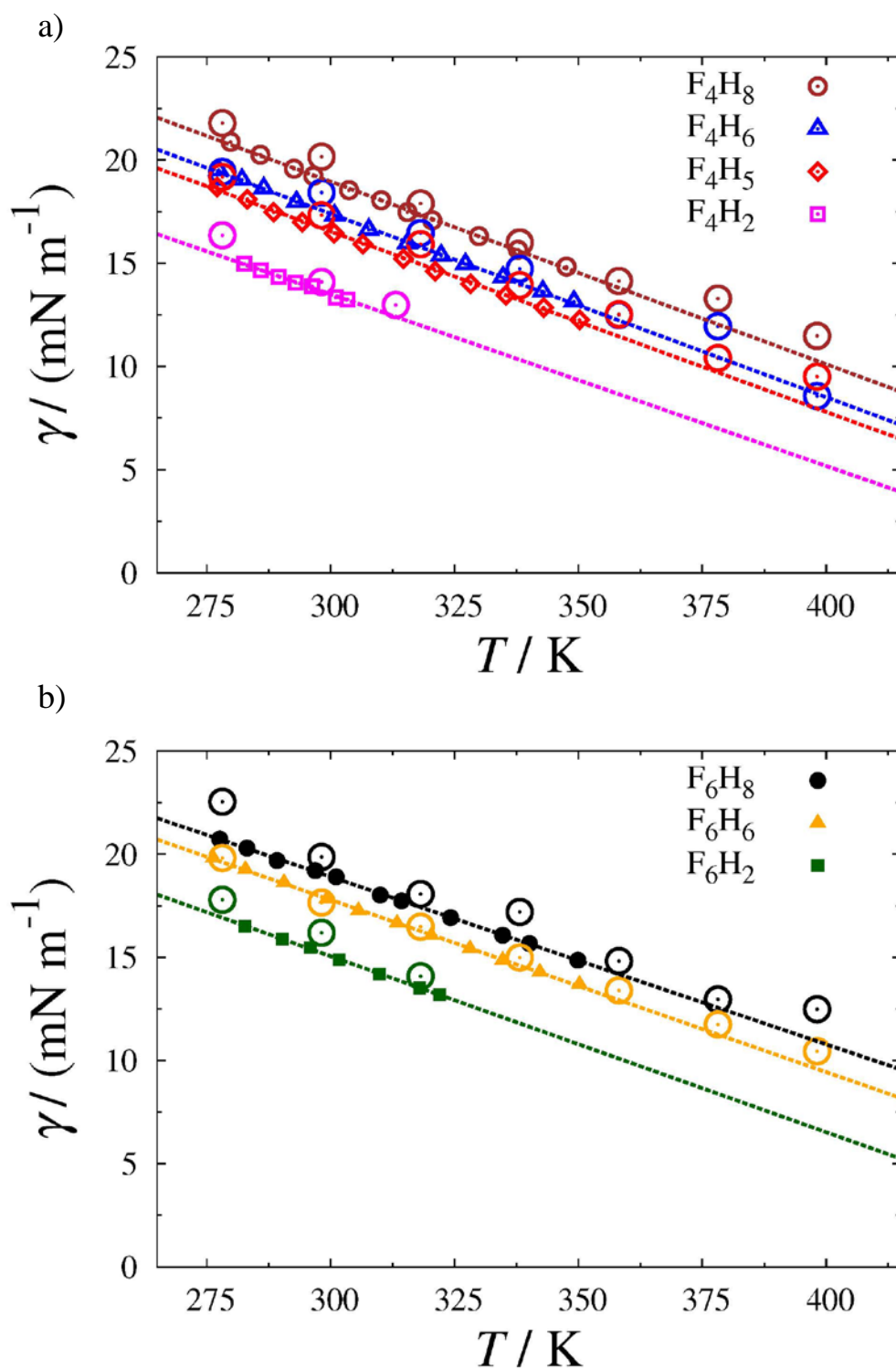


Figure 9. Temperature dependence of the interfacial tension γ for linear perfluoroalkylalkanes F_iH_j : a) F_4H_j with $j = 2, 5, 6,$ and 8 ; b) F_6H_j with $j = 2, 6,$ and 8 . The symbols correspond to the experimental data measured in our current work, the dashed lines are least-square linear fits to the experimental data, and the large open circles denote the predictions obtained with the SAFT- γ Mie CG force field (cf. Table 3) by molecular dynamics simulation.

The interfacial tension simulated with the SAFT- γ Mie CG force field for F_4H_8 and F_6H_6 are compared with the corresponding simulation data for the n -alkane (n -dodecane) and the perfluoro- n -alkane (perfluoro- n -dodecane) of the same chain length in Figure 10. The molecular simulation data are seen to confirm the experimental observation that the interfacial tensions of PFAAs fall between those of n -alkanes and perfluoro- n -alkanes of the same total chain length, being closer to the perfluoro- n -alkane species.

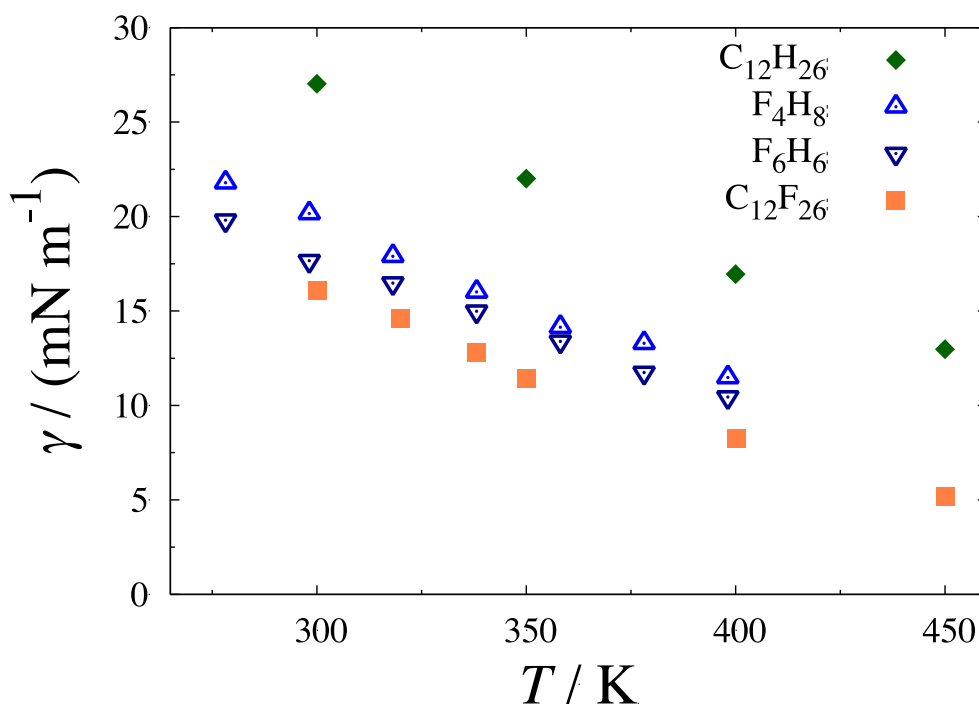


Figure 10. Predictions of the temperature dependence of the interfacial tension obtained with the SAFT- γ Mie CG force field (cf. Table 3) by molecular dynamics simulation for linear C_{12} chain fluids: n -dodecane ($C_{12}H_{26}$), perfluoro- n -dodecane ($C_{12}F_{26}$), and the linear perfluoroalkylalkanes F_4H_8 and F_6H_6 .

Unexpectedly, the interfaces of the four components appear to be of a comparable width (cf. Figure 11). The interfacial density profiles $\rho(z)$ of the linear C_{12} chain fluids as a function of the distance z normal to the interface are compared relative to the density ρ_L of the bulk saturated liquid phase at the same reduced temperature. The interfaces of the PFAA molecules are only slightly wider than their alkane and perfluoroalkane counterparts. The behaviour obtained for other PFAA is similar and is not reported here.

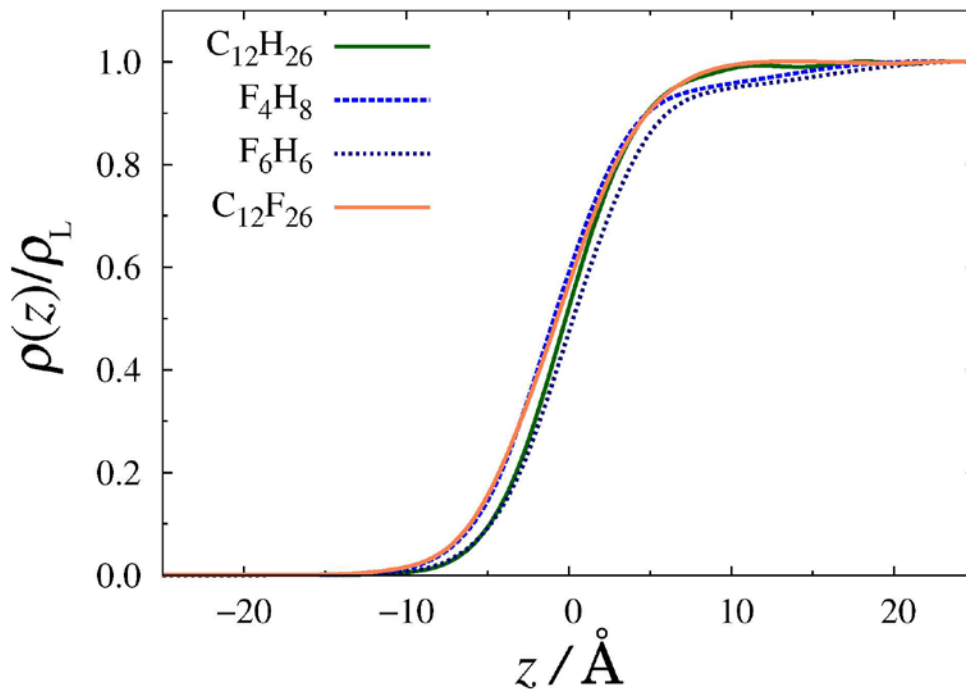


Figure 11. The interfacial density profiles $\rho(z)$ relative to the bulk saturated liquid density ρ_L obtained with the SAFT- γ Mie CG force field (cf. Table 3) by molecular dynamics simulation for C_{12} chain fluids at a reduced temperature of $T_r = 0.55$: *n*-dodecane ($C_{12}H_{26}$), perfluoro-*n*-dodecane ($C_{12}H_{26}$), and the linear perfluoroalkylalkanes F_4H_8 and F_6H_6 .

The F_4H_8 molecule is chosen for further analysis due to its “symmetrical” nature: in our CG mapping, this linear PFAA chain consists of two alkyl (CE, CM), two perfluoroalkyl (FE, FM), and one interconnecting bead (FH). The number density profiles $\rho_B(z) = N_B(z)/(V/\text{\AA}^3)$ (where N_B is the number of beads of a given type) obtained for the separate CG beads of F_4H_8 are depicted in Figure 12. It is apparent that the

perfluorinated groups (FE, FM) accumulate on the vapour side of the interface. The alkyl groups (CE, CM) are found preferentially on the liquid side of the interfacial region, as characterized by the maximum in the profile of the alkyl groups and the complementary minimum in the profile of the perfluorinated groups. The interconnecting segments (FH) exhibit a maximum in the density profile in the intermediate region of the interface. As expected all of the groups are distributed uniformly at the interior of the bulk liquid.

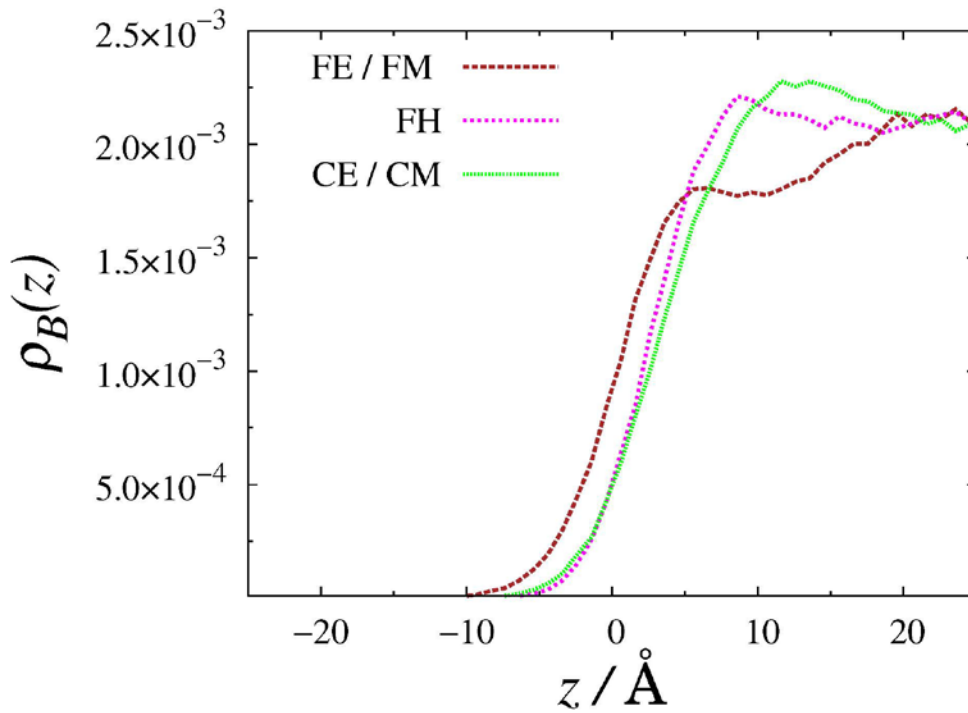


Figure 12. The interfacial density profiles of the CG beads $\rho_B(z) = N_B(z)/(V/\text{\AA}^3)$ of the linear perfluoroalkylalkane F_4H_8 obtained with the SAFT- γ Mie CG force field (cf. Table 3) by molecular dynamics simulation for the alkyl (CE, CM), perfluoroalkyl (FE, FM), and interconnecting (FH) CG beads of at a reduced temperature of $T_r = 0.55$.

The mutual alignment of the molecules can be characterized with the orientational order parameter S_2 , which is calculated from the Saupe order tensor¹³²

$$\mathbf{Q} = \frac{1}{2N} \sum_{i=1}^N (3\hat{u}_i \cdot \hat{u}_i - \mathbf{I}), \quad (14)$$

where \hat{u}_i is the unit vector denoting the orientation of the i th molecule, and \mathbf{I} is the unit tensor. The \mathbf{Q} tensor is then diagonalized and S_2 corresponds to the largest

eigenvalue of the tensor with the director \hat{n} as the corresponding eigenvector. The order parameter provides a measure of the orientation of the molecules around \hat{n} , and runs from zero for randomly oriented to one for perfectly aligned molecules. The unit orientation vector \hat{u}_i of the PFAA molecules is taken as the end-to-end (unit) vector $\hat{r}_{\text{FE-CE}}$ between the centres of mass of the terminal alkyl CE and perfluoroalkyl FE beads. Additional analysis can be performed for the perfluoroalkyl chain vectors $\hat{r}_{\text{FE-FH}}$ and $\hat{r}_{\text{FE-FM}}$ yielding analogous results. It is important to note that one could also consider the principal inertial axis of the molecules as the orientation of the molecule, but we are principally interested in the orientation of the separate chain fragments so the appropriate bead-bead vectors are more suitable in this instance.

The order parameter profile $S_2(z)$ of F_4H_8 determined along the z axis for is shown in Figure 13 a). The complementary density profile (also included in Figure 13) allows one to visualize the location of the interfacial and bulk regions. The interfacial region is characterized by a maximum of the order parameter suggesting a certain level of orientational ordering at the interface, which is slightly higher than in the bulk liquid phase. Quantitatively however, the maximum in the order parameter is $S_2(z) \sim 0.42$, which is far from a system with complete alignment characterized by $S_2(z) = 1.0$.

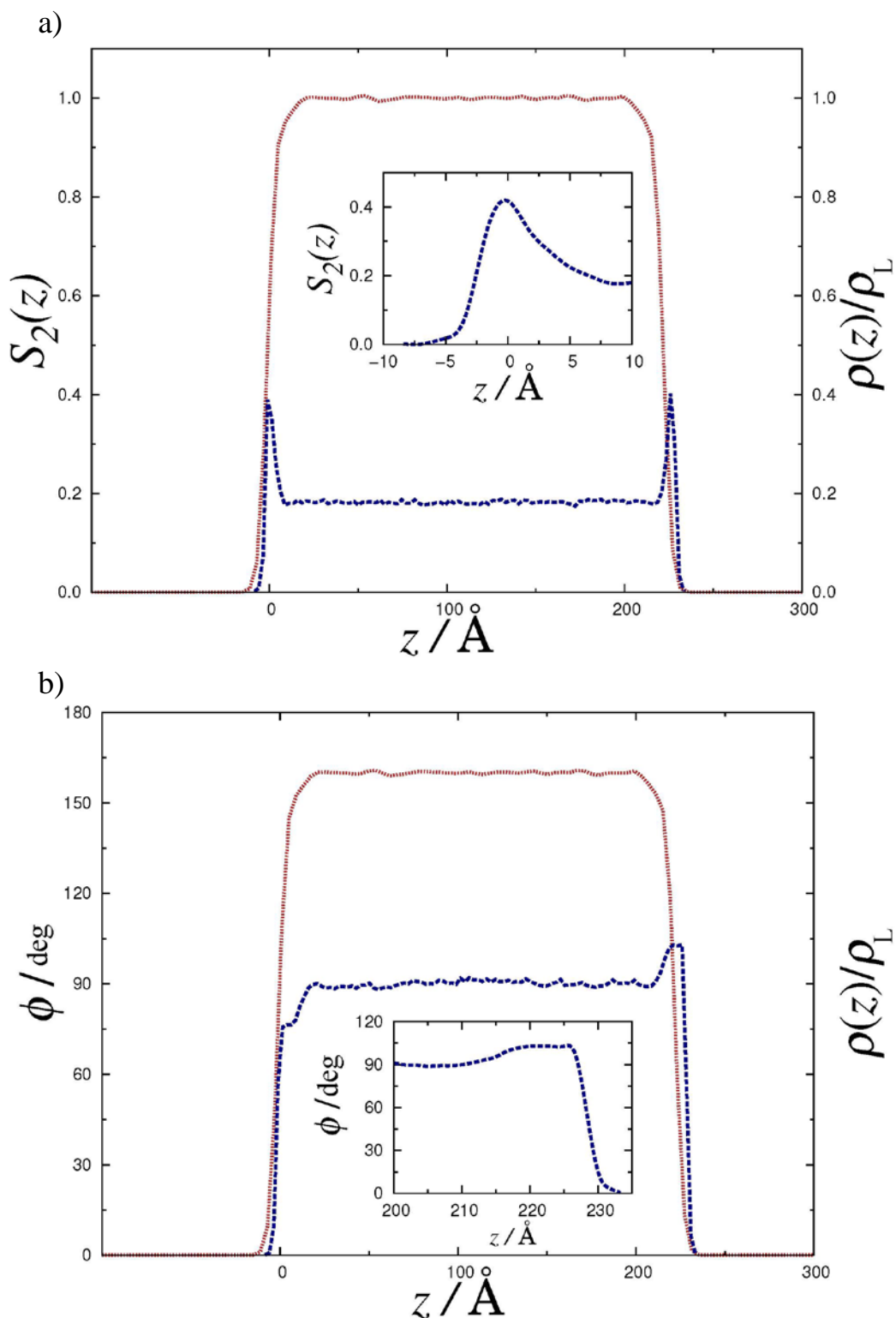


Figure 13. a) The orientational order parameter profile $S_2(z)$ of the end-to-end vector $\hat{\mathbf{r}}_{\text{FE-CE}}$ between the terminal alkyl CE and perfluoroalkyl FE CG beads of the linear perfluoroalkylalkane F_4H_8 obtained with the SAFT- γ Mie CG force field (cf. Table 3) by molecular dynamics simulation at a reduced temperature of $T_r = 0.55$. The complementary density profiles $\rho(z)$ (cf. Figure 11) are also shown as the red dotted curves for completeness. b) The corresponding profile for the average angle ϕ between the end-to-end vector $\hat{\mathbf{r}}_{\text{FE-CE}}$ and the z axis. An enlarged representation of the interfacial region is shown in the insets.

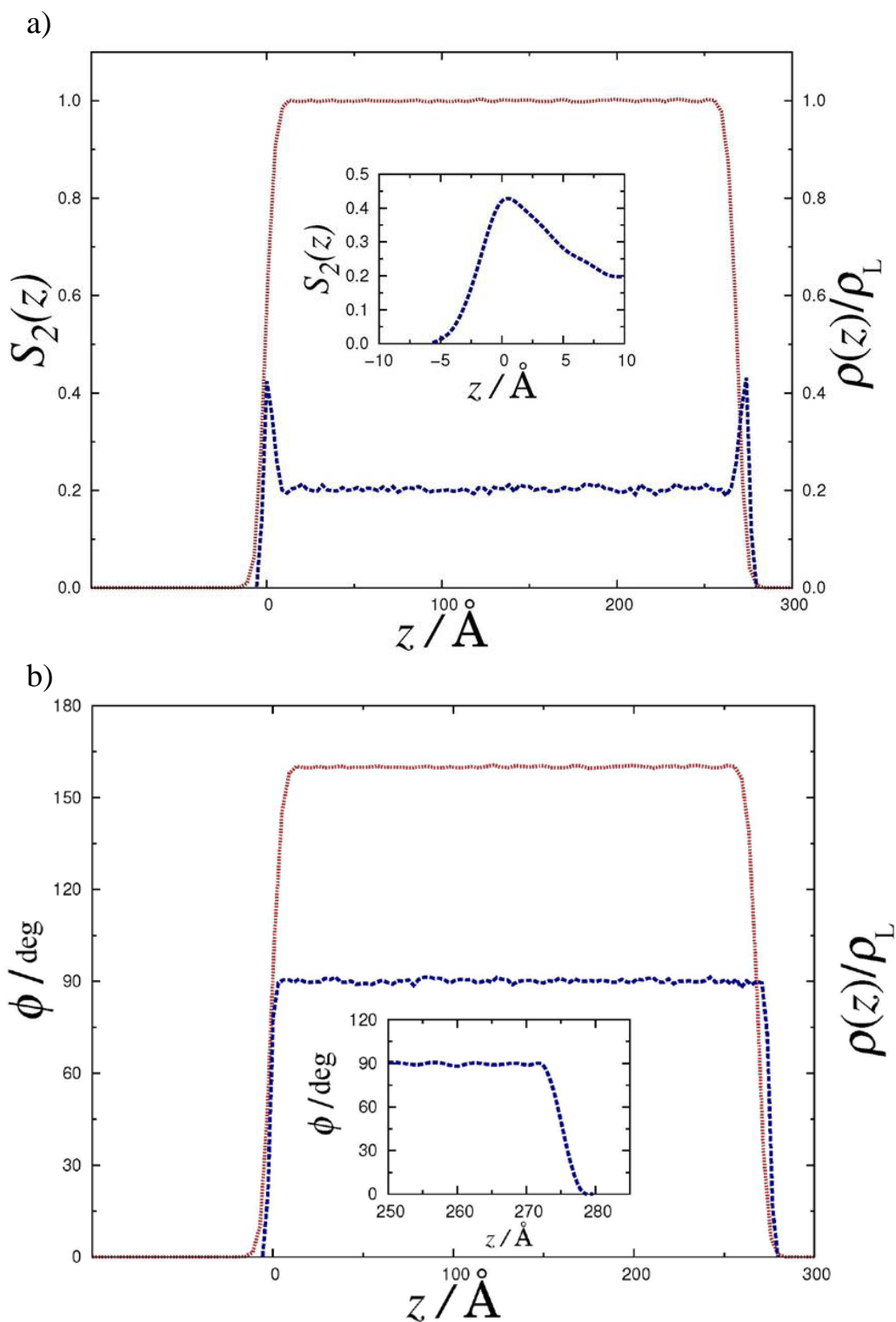


Figure 14. a) The orientational order parameter profile $S_2(z)$ of the end-to-end vector $\hat{\mathbf{r}}_{\text{FE-FE}}$ between the terminal perfluoroalkyl FE CG beads of the fully perfluorinated chain perfluoro-n-dodecane $\text{C}_{12}\text{F}_{26}$ obtained with the SAFT- γ Mie CG force field (cf. Table 3) by molecular dynamics simulation at a reduced temperature of $T_r = 0.55$. The complementary density profiles $\rho(z)$ (cf. Figure 11) are also shown as the red dotted curves for completeness. b) The corresponding profile for the average angle ϕ between the end-to-end vector $\hat{\mathbf{r}}_{\text{FE-FE}}$ and the z axis. An enlarged representation of the interfacial region is shown in the insets.

The orientation of the PFAA chains can be further assessed by calculating the average angle ϕ between the end-to-end vector $\hat{\mathbf{r}}_{\text{FE-CE}}$ and the z axis as a function of the position from the interface. The chains are randomly orientated in the bulk liquid region, corresponding to an average angle of 90° over all orientations ranging from 0° to 180° (cf. Figure 13 b). One can note that the orientational order parameter is not zero but $S_2(z) \sim 0.2$ (cf. Figure 13 a); this is due to system-size effects due to the finite size of the system and binning procedure employed in the analysis¹³³. The interfacial liquid region on the left of Figure 13 b) is characterized by a lowering of the average angle, suggesting that the chains align preferentially along the z axis with the perfluorinated chain ends pointing towards the vapour phase; the angle between $\hat{\mathbf{r}}_{\text{FE-CE}}$ and $\hat{\mathbf{z}}$ tends to 0° . Similarly, the angle in the interfacial region on the right of the figure is seen to exhibit a maximum that can be interpreted as a preferential alignment along the z axis with the perfluorinated chain ends again pointing towards the vapour phase; the angle between $\hat{\mathbf{r}}_{\text{FE-CE}}$ and $\hat{\mathbf{z}}$ now tends to 180° . This observation is consistent with the results from the density profiles observed in Figure 12, suggesting an enrichment of perfluorinated groups at the outer interface.

For comparison, a similar analysis is conducted for a fully perfluorinated compound $\text{C}_{12}\text{F}_{26}$. A maximum in the order parameter can be observed in the interfacial region of Figure 14 a), which suggest an increased alignment of the chains at the interface due to the rigid character of the molecules. However, due to the symmetry of the molecule with no distinction between the right and the left ends, no peaks are observed in the angle profile, characterized by a random orientation in the bulk liquid phase (cf. Figure 14 b).

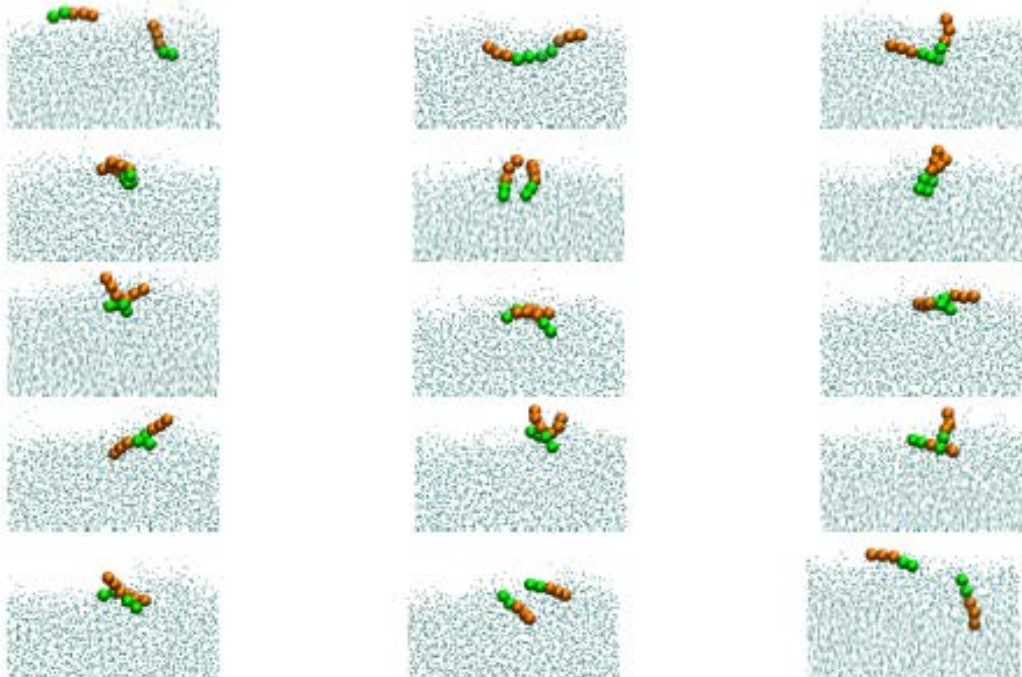


Figure 15. Representative snapshots of the interfacial region obtained by molecular dynamics simulation for the linear perfluoroalkylalkane F_4H_8 with the SAFT- γ Mie CG force field (cf. Table 3) at a reduced temperature of $T_r = 0.55$. Two random molecules are highlighted and followed at different times, separated by 0.02 ns. The perfluoro groups are shown in orange, alkyl groups are in green.

Snapshots of selected configurations for a pair of randomly chosen F_4H_8 molecules close to the liquid-vapour interface during the course of a typical simulation run are shown in Figure 15. Neither the alignment nor the orientation of the molecules is found to be very pronounced.

In conclusion, the MD simulation results suggest that the PFAA chains tend to align perpendicular to the interface with the perfluoro-groups accumulating at the outer interface region. Similar findings were obtained by Hariharan and Harris¹⁷ and by Pierce *et al.*¹⁸ from the molecular simulations of the PFAA molecules based on more detailed atomistic force fields.

5. Conclusions

The surface tensions of seven linear perfluoroalkylalkanes (F_4H_2 , F_4H_5 , F_4H_6 , F_4H_8 , F_6H_2 , F_6H_6 , F_6H_8) are experimentally determined over a wide temperature range (276 to 350 K). The corresponding surface thermodynamic functions and the critical temperatures of the PFAA compounds are estimated from the temperature dependence of the surface tension. A CG force field is developed for these systems based on a top-down parametrization performed by estimating the intermolecular interactions from the experimental densities and vapour pressures using the SAFT- γ EoS³⁷.

While it is tempting to try to compare the results with those of *n*-alkanes, perfluoro-*n*-alkanes and their mixtures, this has proven to be a far from trivial task. At a very gross scale, the expected values of interfacial tensions lie between those of alkanes and perfluoroalkanes. However, PFAA possess distinct thermophysical properties, most likely a result of the presence of the unique bond that links the perfluoroalkyl chain to the alkyl chain. The resulting permanent dipole moment between the two coexisting chemical moieties has significant implications in the surface tension of PFAA. Furthermore, the properties of the interfacial region are dominated by the tendency of the molecules to align perpendicular to the interface with the perfluorinated groups accumulating at the outer interface.

Acknowledgements

P.M. and E.J.M.F. acknowledge funding from Fundação para a Ciência e a Tecnologia, in the form of Grants SFRH/BPD/81748/2011 and UID/QUI/00100/2013. O.L. is very grateful to Imperial College London for a Research Excellence Award which supported her PhD studies. G.J. and E.A.M. also gratefully acknowledge additional funding to the Molecular Systems Engineering Group from the Engineering and Physical Sciences Research Council (EPSRC) of the UK (Grant Nos. GR/T17595, GR/N35991, EP/E016340, and EP/J014958), the Joint Research Equipment Initiative (JREI) (Grant No. GR/M94426), and the Royal Society-Wolfson Foundation refurbishment scheme. Support from the Thomas Young Centre for Theory and Simulation of Materials through grant TYC-101 is acknowledged. The simulations described herein were performed using the facilities of the Imperial College High-Performance Computing Service.

Supplemental Material

A downloadable file with experimental liquid densities of the linear perfluoroalkylalkanes perfluorobutylethane (F4H2) and perfluorohexylethane (F6H2) is available from Supplemental Material link from the article home page.

References

-
- ¹ Broniatowski, M.; Dynarowicz-Łątka, P. Semifluorinated Alkanes - Primitive Surfactants of Fascinating Properties. *Adv. Colloid Interface Sci.*, **2008**, *138*, 63–83.
- ² Turberg, M.P.; Brady, J.E. Semifluorinated Hydrocarbons – Primitive Surfactant Molecules. *J. Am. Chem. Soc.*, **1988**, *110*, 7797–7801.
- ³ Binks, B. P.; Fletcher, P. D. I.; Kotsev, S. N.; Thompson, R. L. Adsorption and aggregation of semifluorinated alkanes in binary and ternary mixtures with hydrocarbon and fluorocarbon solvents. *Langmuir*, **1997**, *13*, 6669–6682.
- ⁴ Mahler, W.; Guillon, D.; Skoulios, A. Smectic Liquid-Crystal from (Perfluorododecyl) Decane. *Mol. Cryst. Liq. Cryst.*, **1985**, *2*, 111–119.
- ⁵ Viney, C.; Russell, T. P.; Depero, L. E.; Twieg, R. J. Transitions to Liquid-Crystalline Phases in a Semifluorinated Alkane. *Mol. Cryst. Liq. Cryst.* **1989**, *168*, 63–82.
- ⁶ Viney, C.; Twieg, R. J.; Russell, T. P.; Depero, L. E.

The Structural Basis of Transitions Between Highly Ordered Smectic Phases in Semifluorinated Alkanes. *Liq. Cryst.*, **1989**, *5*, 1783–1788.

⁷ Maaloum, M.; Muller, P.; Krafft, M. P.

Monodisperse Surface Micelles of Nonpolar Amphiphiles in Langmuir Monolayers. *Angew. Chem. Int. Ed.*, **2002**, *41*, 4331–4334.

⁸ Simões Gamboa, A. L.; Filipe, E. J. M.; Brogueira, P.

Nanoscale Pattern Formation in Langmuir–Blodgett Films of a Semifluorinated Alkane and a Polystyrene–Poly(Ethylene Oxide) Diblock Copolymer. *Nano Lett.*, **2002**, *2*, 1083–1086.

⁹ Rabolt, J. F.; Russell, T. P.; Twieg, R. J.

Structural Studies of Semifluorinated N-Alkanes. 1. Synthesis and Characterization of F(CF₂)_n(CH₂)_mH in the Solid State.

Macromolecules, **1984**, *17*, 2786–2794.

¹⁰ Russell, T. P.; Rabolt, J. F.; Twieg, R. J.; Siemens, R. L.; Farmer, B. L.

Structural Characterization of Semifluorinated N-Alkanes. 2. Solid-Solid Transition Behavior. *Macromolecules*, **1986**, *19*, 1135–1143.

¹¹ Höpken, J.; Möller, M.

On the Morphology of (perfluoroalkyl)alkanes.

Macromolecules **1992**, *25*, 2482–2489.

¹² Marczuk, P.; Lang, P.

A Structural X-ray Study on Semifluorinated Alkanes (SFA): SFA revisited.

Macromolecules, **1998**, *31*, 9013–9018.

¹³ Gang, O.; Ellmann, J.; Möller, M.; Kraack, H.; Sirota, E.B.; Ocko, B.M.; Deutsch, M.

Surface Phases of Semi-Fluorinated Alkane Melts.

Europhys. Lett., **2000**, *49*, 761–767.

¹⁴ Sloutskin, E.; Kraack, H.; Ocko, B.; Ellmann, J.; Möller, M.; Lo Nostro, P.; Deutsch, M.

Thermal Expansion of Surface-Frozen Monolayers of Semifluorinated Alkanes.

Langmuir, **2002**, *18*, 1963–1967.

¹⁵ Tsagogiorgas, C.; Krebs, J.; Pukelsheim, M.; Beck, G.; Yard, B.; Theisinger, B.; Quintel, M.; Luecke, T.

Semifluorinated Alkanes – A New Class of Excipients Suitable for Pulmonary Drug Delivery.

Eur. J. Pharm. Biopharm., **2010**, *76*, 75–82.

¹⁶ McLain, S. J.; Sauer, B. B.; Firment, L. E.

Surface Properties and Metathesis Synthesis of Block Copolymers Including Perfluoroalkyl-Ended Polyethylenes.

Macromolecules, **1996**, *29*, 8211–8219.

¹⁷ Hariharan, A.; Harris, J. G.

Structure and Thermodynamics of the Liquid–vapour Interface of Fluorocarbons and Semifluorinated Alkane Diblocks: A Molecular Dynamics Study.

J. Chem. Phys., **1994**, *101*, 4156–4165.

¹⁸ Pierce, F.; Tsige, M.; Borodin, O.; Perahia, D.; Grest, G. S.

Interfacial Properties of Semifluorinated Alkane Diblock Copolymers.

J. Chem. Phys., **2008**, *128*, 214903.

¹⁹ Pádua, A. A. H.

Torsion Energy Profiles and Force Fields Derived from Ab Initio Calculations for Simulations of Hydrocarbon–Fluorocarbon Diblocks and Perfluoroalkylbromides.

J. Phys. Chem. A, **2002**, *106*, 10116–10123.

²⁰ Borodin, O.; Smith, G. D.; Bedrov, D.

A Quantum Chemistry Based Force Field for Perfluoroalkanes and Poly(tetrafluoroethylene).

J. Phys. Chem. B, **2002**, *106*, 9912–9922.

²¹ Shin, S.; Collazo, N.; Rice, S. A.

A Molecular-Dynamics Study of the Packing Structures in Monolayers of Partially Fluorinated Amphiphiles.

J. Chem. Phys., **1992**, *96*, 1352–1366.

²² Cui, S. T.; Siepmann, J. I.; Cochran, H. D.; Cummings, P. T.

Intermolecular Potentials and Vapor–liquid Phase Equilibria of Perfluorinated Alkanes.
Fluid Phase Equilib., **1998**, *146*, 51–61.

²³ Jorgensen, W. L.; Maxwell, D. S.; Tirado-Rives, J.
Development and Testing of the OPLS All-Atom Force Field on Conformational Energetics and Properties of Organic Liquids.
J. Am. Chem. Soc., **1996**, *118*, 11225–11236.

²⁴ Watkins, E. K.; Jorgensen, W. L.
Perfluoroalkanes: Conformational Analysis and Liquid-State Properties from Ab Initio and Monte Carlo Calculations.
J. Phys. Chem. A, **2001**, *105*, 4118–4125.

²⁵ Potoff, J. J.; Bernard-Brunel, D. A.
Mie Potentials for Phase Equilibria Calculations: Application to Alkanes and Perfluoroalkanes.
J. Phys. Chem. B, **2009**, *113*, 14725–14731.

²⁶ Amat, M. A.; Rutledge, G. C.
Liquid-Vapor Equilibria and Interfacial Properties of n-Alkanes and Perfluoroalkanes by Molecular Simulation.
J. Chem. Phys., **2010**, *132*, 114704.

²⁷ Dominguez, H., Haslam, A. J., Jackson, G., Müller, E. A.
Modelling and Understanding of the Vapour–Liquid and Liquid–Liquid Interfacial Properties for the Binary Mixture of n-Heptane and Perfluoro-n-Hexane **2013**.
J. Mol. Liq., *185*, 36–43.

²⁸ Paulechka, E., Kroenlein, K., Kazakov, A., Frenkel, M.
A Systematic Approach for Development of an OPLS-Like Force Field and Its Application to Hydrofluorocarbons.
J. Phys. Chem. B, **2012**, *116*, 14389–14397.

²⁹ Lachet, V., Teuler, J. M., Rousseau, B.
Classical Force Field for Hydrofluorocarbon Molecular Simulations. Application to the Study of Gas Solubility in Poly(vinylidene fluoride).
J. Phys. Chem. A, **2015**, *119*, 140–151.

³⁰ Nielsen, S., Lopez, C., Srinivas, G., Klein, M.
Coarse Grain Models and the Computer Simulation of Soft Materials.
J. Phys. Condens. Matter, **2004**, *16*, R481–R512.

³¹ Saunders, M. G., Voth, G. A.
Coarse-Graining Methods for Computational Biology.
Ann. Rev. Biophysics, **2013**, *42*(1), 73–93.

³² Reith, D.; Putz, M.; Müller-Plathe, F.
Deriving Effective Mesoscale Potentials from Atomistic Simulations.
J. Comput. Chem., **2003**, *24*, 1624–1636.

³³ Izvekov, S.; Voth, G. A.
A Multiscale Coarse-Graining Method for Biomolecular Systems.
J. Phys. Chem. B, **2005**, *109*, 2469–2473.

³⁴ Lyubartsev, A. P.; Laaksonen, A.
Calculation of Effective Interaction Potentials from Radial-Distribution Functions – A Reverse Monte Carlo Approach.
Phys. Rev. E, **1995**, *52*, 3730–3737.

³⁵ Noid, W. G.
Perspective: Coarse-Grained Models for Biomolecular Systems.
J. Chem. Phys., **2013**, *139*, 090901.

³⁶ Brini, E.; Algaer, E. A.; Ganguly, P.; Li, C. L.; Rodriguez-Ropero, F.; van der Vegt, N. F. A.
Systematic Coarse-Graining Methods for Soft Matter Simulations - A Review.
Soft Matter, **2013**, *9*, 2108–2119.

³⁷ Papaioannou, V.; Lafitte, T.; Avendaño, C.; Adjiman, C. S.; Jackson, G.; Müller, E. A.; Galindo, A.
Group Contribution Methodology Based on the Statistical Associating Fluid Theory for Heteronuclear Molecules Formed from Mie Segments.
J. Chem. Phys., **2014**, *140*, 054107.

³⁸ Lymperiadis, A.; Adjiman, C. S.; Galindo, A.; Jackson, G.

A Group Contribution Method for Associating Chain Molecules Based on the Statistical Associating Fluid Theory (SAFT- γ).

J. Chem. Phys., **2007**, *127*, 234903.

³⁹ Lymeriadis, A.; Adjiman, C. S.; Jackson, G.; Galindo, A.

A Generalisation of the SAFT-Group Contribution Method for Groups Comprising Multiple Spherical Segments.

Fluid Phase Equilib., **2008**, *274*, 85–104.

⁴⁰ Lafitte, T.; Apostolakou, A.; Avendaño, C.; Galindo, A.; Adjiman, C. S.; Müller, E. A.; Jackson, G.

Accurate Statistical Associating Fluid Theory for Chain Molecules Formed from Mie Segments.

J. Chem. Phys., **2013**, *139*, 154504.

⁴¹ Chapman, W. G.; Gubbins, K. E.; Jackson, G.; Radosz, M.

SAFT – Equation-of-State Solution Model for Associating Fluids.

Fluid Phase Equilib., **1989**, *52*, 31–38.

⁴² Chapman, W. G.; Gubbins, K. E.; Jackson, G.; Radosz, M.

New Reference Equation of State for Associating Liquids.

Ind. Eng. Chem. Res., **1990**, *29*, 1709–1721.

⁴³ Gil-Villegas, A.; Galindo, A.; Whitehead, P. J.; Mills, S. J.; Jackson, G.; Burgess, A. N.

Statistical Associating Fluid Theory for Chain Molecules with Attractive Potentials of Variable Range.

J. Chem. Phys., **1997**, *106*, 4168–4186.

⁴⁴ Galindo, A.; Davies, L. A.; Gil-Villegas, A.; Jackson, G.

The Thermodynamics of Mixtures and the Corresponding Mixing Rules in the SAFT-VR Approach for Potentials of Variable Range.

Mol. Phys., **1998**, *93*, 241-252.

⁴⁵ Avendaño, C.; Lafitte, T.; Galindo, A.; Adjiman, C. S.; Jackson, G.; Müller, E. A.

SAFT- γ Force Field for the Simulation of Molecular Fluids. 1. A Single-Site Coarse Grained Model of Carbon Dioxide.

J. Phys. Chem. B, **2011**, *115*, 11154–11169.

⁴⁶ Aimoli, C. G.; Maginn, E. J.; Abreu, C. R. A.

Thermodynamic Properties of Supercritical Mixtures of Carbon Dioxide and Methane: A Molecular Simulation Study.

J. Chem. Eng. Data, **2014**, *59*, 3041–3054.

⁴⁷ Aimoli, C. G.; Maginn, E. J.; Abreu, C. R. A.

Transport Properties of Carbon Dioxide and Methane from Molecular Dynamics Simulations.

J. Chem. Phys., **2014**, *141*, 134101.

⁴⁸ Avendaño, C.; Lafitte, T.; Adjiman, C. S.; Galindo, A.; Müller, E. A.; Jackson, G.

SAFT- γ Force Field for the Simulation of Molecular Fluids: 2. Coarse-Grained Models of Greenhouse Gases, Refrigerants, and Long Alkanes.

J. Phys. Chem. B, **2013**, *117*, 2717–2733.

⁴⁹ Lafitte, T.; Avendaño, C.; Papaioannou, V.; Galindo, A.; Adjiman, C. S.; Jackson, G.; Müller, E. A.

SAFT- γ Force Field for the Simulation of Molecular Fluids: 3. Coarse-Grained Models of Benzene and Hetero-Group Models of N-Decylbenzene.

Mol. Phys., **2012**, *110*, 1189–1203.

⁵⁰ Lobanova, O.; Avendaño, C.; Lafitte, T.; Müller, E. A.; Jackson, G.

SAFT- γ Force Field for the Simulation of Molecular Fluids: 4. A Single-Site Coarse-Grained Model of Water Applicable over a Wide Temperature Range.

Mol. Phys., **2015**, *113*, 1228–1249.

⁵¹ Müller, E. A.; Mejía, A.

Resolving Discrepancies in the Measurements of the Interfacial Tension for the CO₂ + H₂O Mixture by Computer Simulation.

J. Phys. Chem. Lett., **2014**, *5*, 1267–1271.

⁵² Míguez, J. M.; Garrido, J. M.; Blas, F. J.; Segura, H.; Mejía, A.; Piñeiro, M. M.

Comprehensive Characterization of Interfacial Behavior for the Mixture CO₂+ H₂O+ CH₄: Comparison between Atomistic and Coarse Grained Molecular Simulation Models and Density Gradient Theory.

J. Chem. Phys. C, **2014**, *118*, 24504–24519.

⁵³ Lobanova, O.; Mejía, A.; Jackson, G.; Müller, E. A.

SAFT- γ Force Field for the Simulation of Molecular Fluids 6: Binary and Ternary Mixtures Comprising Water, Carbon Dioxide, and n-Alkanes.
J. Chem. Thermo., **2016**, *93*, 320–336.

⁵⁴ Rahman, S.; Lobanova, O.; Jiménez, M. G.; Avendaño, C.; Braga, C.; Raptis, V.; Müller, E. A.; Jackson, G.; Galindo, A.
in preparation, (2016).

⁵⁵ Lobanova, O.; Herdes, C.; Jackson, G.; Muller, E. A.
in preparation (2016).

⁵⁶ Herdes, C.; Santiso, E. E.; James, C.; Eastoe, J.; Müller, E. A.
Modelling the Interfacial Behaviour of Dilute Light-Switching Surfactant Solutions.
J. Colloid Interf. Sci., **2015**, *445*, 16–23.

⁵⁷ Theodorakis, P. E.; Müller, E. A.; Craster, R. V.; Matar, O. K.
Superspreading: Mechanisms and Molecular Design.
Langmuir, **2015**, *31*, 2304–2309.

⁵⁸ Mejía, A., Herdes, C., Müller, E. A.
Force Fields for Coarse-Grained Molecular Simulations from a Corresponding States Correlation.
Ind. Eng. Chem. Res., **2014**, *53*, 4131–4141.

⁵⁹ Müller, E. A.; Jackson, G.
Force-Field Parameters from the SAFT- γ Equation of State for Use in Coarse-Grained Molecular Simulations.
Annu. Rev. Chem. Biomol. Eng., **2014**, *5*, 405–427.

⁶⁰ Nielsen, S., Lopez, C., Srinivas, G., Klein, M.
A coarse grain model for n-alkanes parameterized from surface tension data.
J. Chem. Phys., **2003**, *119*, 7043–7049.

⁶¹ Chiu, S.-W., Scott, H. L., Jakobsson, E.
A Coarse-Grained Model Based on Morse Potential for Water and n-Alkanes.
J. Chem. Theory Comput., **2010**, *6*, 851–863.

⁶² Marrink, S. J., Risselada, H. J., Yefimov, S., Tieleman, D. P., De Vries, A. H.
The MARTINI Force Field: Coarse Grained Model for Biomolecular Simulations.
J. Phys. Chem. B, **2007**, *111*, 7812–7824.

⁶³ Maerzke, K.A.; Siepmann, J.I.
Transferable Potentials for Phase Equilibria– Coarse-Grain Description for Linear Alkanes.
J. Phys. Chem. B, **2011**, *115*, 3452–3465.

⁶⁴ Du, Q., Yang, Z., Yang, N., Yang, X.
Coarse-Grained Model for Perfluorocarbons and Phase Equilibrium Simulation of Perfluorocarbons/CO₂ Mixtures. *Ind. Eng. Chem. Res.*, **2010**, *49*, 8271–8278.

⁶⁵ Herdes, C; Forte, E; Jackson, G.; Müller, E.A.
Predicting the adsorption of n-perfluorohexane in BAM P109 standard activated carbon by molecular simulation using SAFT- γ Mie coarse-grained force fields.
Adsorpt. Sci. Tech., **2016**, *34*, 64–78.

⁶⁶ Archer, A. L.; Amos, M. D.; Jackson, G.; McLure, I. A.
The theoretical prediction of the critical points of alkanes, perfluoroalkanes, and their mixtures using bonded hard-sphere (BHS) theory.
Int. J. Thermophys., **1996**, *17*, 201–211.

⁶⁷ Clements, P. J.; Zafar, S.; Galindo, A.; Jackson, G.; McLure, I. A.
Thermodynamics of Ternary Mixtures Exhibiting Tunnel Phase Behaviour Part 3. Hexane–Hexamethyldisiloxane–Perfluorohexane.
J. Chem. Soc., Faraday Trans., **1997**, *93*, 1331–1339.

⁶⁸ McCabe, C.; Galindo, A.; Gil-Villegas, A.; Jackson, G.
Predicting the High-Pressure Phase Equilibria of Binary Mixtures of Perfluoro-n-Alkanes + n-Alkanes Using the SAFT-VR Approach.
J. Phys. Chem. B, **1998**, *102*, 8060–8069.

⁶⁹ Morgado, P.; McCabe, C.; Filipe, E. J. M.
Modelling the Phase Behaviour and Excess Properties of Alkane + Perfluoroalkane Binary Mixtures with the SAFT–VR Approach.
Fluid Phase Equilib., **2005**, *228*, 389–393.

-
- ⁷⁰ Pratas De Melo, M. J.; Dias, A. M. A.; Blesic, M.; Rebelo, L. P. N.; Vega, L. F.; Coutinho, J. A. P.; Marrucho, I. M.
Liquid-liquid Equilibrium of (perfluoroalkane+alkane) Binary Mixtures.
Fluid Phase Equilib., **2006**, *242*, 210–219.
- ⁷¹ Aparicio, S.
Phase Equilibria in Perfluoroalkane + Alkane Binary Systems from PC-SAFT Equation of State.
J. Supercrit. Fluids, **2008**, *46*, 10–20.
- ⁷² Dos Ramos, M. C.; Blas, F. J.
Theory of Phase Equilibria for Model Mixtures of n-Alkanes, Perfluoroalkanes and Perfluoroalkylalkane Diblock Surfactants.
Mol. Phys., **2007**, *105*, 1319–1334.
- ⁷³ Morgado, P.; Zhao, H.; Blas, F. J.; McCabe, C.; Rebelo, L. P. N.; Filipe, E. J. M.
Liquid Phase Behavior of Perfluoroalkylalkane Surfactants.
J. Phys. Chem. B, **2007**, *111*, 2856–2863.
- ⁷⁴ Morgado, P.; Lewis, J. B.; Laginhas, C. M. C.; Martins, L. F. G.; McCabe, C.; Blas, F. J.; Filipe, E. J. M.
Systems Involving Hydrogenated and Fluorinated Chains: Volumetric Properties of Perfluoroalkanes and Perfluoroalkylalkane Surfactants.
J. Phys. Chem. B, **2011**, *115*, 15013–15023.
- ⁷⁵ Morgado, P.; Das, G.; McCabe, C.; Filipe, E. J. M.
Vapor Pressure of Perfluoroalkylalkanes: The Role of the Dipole.
J. Phys. Chem. B, **2015**, *119*, 1623–1632.
- ⁷⁶ Morgado, P.; Tomás, R.; Zhao, H.; Dos Ramos, M. C.; Blas, F. J.; McCabe, C.; Filipe, E. J. M.
Solution Behavior of Perfluoroalkanes and Perfluoroalkylalkane Surfactants in N-Octane.
J. Phys. Chem. C, **2007**, *111*, 15962–15968.
- ⁷⁷ Morgado, P.; Rodrigues, H.; Blas, F. J.; McCabe, C.; Filipe, E. J. M.
Perfluoroalkanes and Perfluoroalkylalkane Surfactants in Solution: Partial Molar Volumes in N-Octane and Hetero-SAFT-VR Modelling.
Fluid Phase Equilib., **2011**, *306*, 76–81.
- ⁷⁸ Peng, Y.; Zhao, H.; McCabe, C.
On the Thermodynamics of Diblock Chain Fluids from Simulation and Heteronuclear Statistical Associating Fluid Theory for Potentials of Variable Range.
Mol. Phys., **2006**, *104*, 571–586.
- ⁷⁹ Gloor, G. J.; Jackson, G.; Blas, F. J.; del Rio, E. M.; de Miguel, E.
An Accurate Density Functional Theory for the Vapor-Liquid Interface of Associating Chain Molecules Based on the Statistical Associating Fluid Theory for Potentials of Variable Range.
J. Chem. Phys., **2004**, *121*, 12740–12759.
- ⁸⁰ Gloor, G. J.; Jackson, G.; Blas, F. J.; del Rio, E. M.; de Miguel, E.
Prediction of the Vapor-Liquid Interfacial Tension of Nonassociating and Associating Fluids with the SAFT-VR Density Functional Theory.
J. Phys. Chem. C, **2007**, *111*, 15513–15522.
- ⁸¹ Llovel, F.; Galindo, A.; Blas, F. J.; Jackson, G.
Classical Density Functional Theory for the Prediction of the Surface Tension and Interfacial Properties of Fluids Mixtures of Chain Molecules Based on the Statistical Associating Fluid Theory for Potentials of Variable Range.
J. Chem. Phys., **2010**, *133*, 024704.
- ⁸² Cumicheo, C.; Cartes, M.; Segura, H.; Müller, E. A.; Mejía, A.
High-Pressure Densities and Interfacial Tensions of Binary Systems Containing Carbon Dioxide+n-Alkanes:(n-Dodecane, n-Tridecane, n-Tetradecane).
Fluid Phase Equilib., **2014**, *380*, 82–92.
- ⁸³ Chow, Y. T. F.; Eriksen, D. K.; Galindo, A.; Haslam, A. J.; Jackson, G.; Maitland, G. C.; Trusler, J. P. M.
Interfacial Tensions of Systems Comprising Water, Carbon Dioxide and Diluent Gases at High Pressures: Experimental Measurements and Modelling with SAFT-VR Mie and Square-Gradient Theory.
Fluid Phase Equilib., **2016**, *407*, 159–176.
- ⁸⁴ Hoorfar, M.; Neumann, A. W.
Recent Progress in Axisymmetric Drop Shape Analysis (ADSA).
Adv. Colloid Interface Sci., **2006**, *121*, 25–49.

-
- ⁸⁵ Hoorfar, M.; Kurz, M. A.; Neumann, A. W.
Evaluation of the Surface Tension Measurement of Axisymmetric Drop Shape Analysis (ADSA) Using a Shape Parameter.
Colloids Surf. A Physicochem. Eng. Asp., **2005**, *260*, 277–285.
- ⁸⁶ Jasper, J. J.
The Surface Tension of Pure Liquid Compounds.
J. Phys. Chem. Ref. Data, **1972**, *1*, 841–1009.
- ⁸⁷ Korosi, G.; Kovats, E. S.
Density and Surface Tension of 83 Organic Liquids.
J. Chem. Eng. Data, **1981**, *26*, 323–332.
- ⁸⁸ Stiles, V. E.; Cady, G. H.
Physical Properties of Perfluoro-n-Hexane and Perfluoro-2-Methylpentane.
J. Am. Chem. Soc., **1952**, *74*, 3771–3773.
- ⁸⁹ McLure, I. A.; Soares, V. A. M.; Edmonds, B.
Surface Tension of Perfluoropropane, Perfluoro-n-Butane, Perfluoro-n-Hexane, Perfluoro-Octane, Perfluorotributylamine and n-Pentane. Application of the Principle of Corresponding States to the Surface Tension of Perfluoroalkanes.
J. Chem. Soc., Faraday Trans. 1, **1982**, *78*, 2251–2257.
- ⁹⁰ Nishikido, N.; Mahler, W.; Mukerjee, P.
Interfacial Tensions of Perfluorohexane and Perfluorodecalin against Water.
Langmuir, **1989**, *5*, 227–229.
- ⁹¹ Haslam, A. J.; Galindo, A.; Jackson, G.
Prediction of Binary Intermolecular Potential Parameters for Use in Modelling Fluid Mixtures.
Fluid Phase Equilib., **2008**, *266*, 105–128.
- ⁹² Vrabec, J.; Stoll, J.; Hasse, H.
Molecular Models of Unlike Interactions in Fluid Mixtures.
Mol. Sim., **2005**, *31*, 215–221.
- ⁹³ Bedford, R. G.; Dunlap, R. D.
Solubilities and Volume Changes Attending Mixing for the System: Perfluoro-n-hexane – n-Hexane.
J. Am. Chem. Soc., **1958**, *80*, 282–285.
- ⁹⁴ Kreglewski, A.
Miscibility of n-Octane with some Perfluoro-Compounds. The Shape of the Coexistence Curve in the Critical Region.
Bull. Acad. Polon. Sci. Ser. Sci. Chim., **1963**, *11*, 91–96.
- ⁹⁵ Block, T. E.; Judd, N. F.; McLure, I. A.; Knobler, C. M.; Scott, R. L.
Excess Volumes in the Critical Solution Region.
J. Phys. Chem., **1981**, *8*, 3282–3290.
- ⁹⁶ Schmelzer, J.; Alekseeva, M. V.
Vapor-liquid and Liquid-Liquid Equilibria in Systems Made up of n-Hexane, n-Perfluorohexane and n-Propanol. Part I. Binary Systems.
Chem. Tech. (Leipzig), **1982**, *34*, 424–426.
- ⁹⁷ Skripov, V. P.; Faizullin, M. Z.
Thermodynamic similarity of phase-separating binary liquid mixtures having an upper critical temperature.
J. Chem. Thermo., **1989**, *21*, 687–700.
- ⁹⁸ McLure, I. A.; Clements, P. J.
Shear Viscosity of Hexane + Tetradecafluorohexane Near the Upper Critical Endpoint.
Ber. Bunsen-Ges., **1997**, *101*, 114–119.
- ⁹⁹ Duce, C.; Tine, M. R.; Lepori, L.; Matteoli, E.
VLE and LLE of Perfluoroalkane + Alkane Mixtures.
Fluid Phase Equilib., **2002**, *199*, 197–212.
- ¹⁰⁰ Lo Nostro, P.; Scalise, L.; Baglioni, P.
Phase Separation in Binary Mixtures Containing Linear Perfluoroalkanes.
J. Chem. Eng. Data, **2005**, *50*, 1148–1152.
- ¹⁰¹ Khairulin, R. A.; Stankus, S. V.; Gruzdev, V. A.

-
- Liquid-Liquid Coexistence Curve of n-Perfluorohexane – n-Hexane System.
Int. J. Thermophys., **2007**, *28*, 1245–1254.
- ¹⁰² Matsuda, H.; Kitabatake, A.; Kosuge, M.; Kurihara, K.; Tochigi, K.; Ochi, K.
Liquid-Liquid Equilibrium Data for Binary Perfluoroalkane (C6 and C8) + n-Alkane Systems.
Fluid Phase Equilib., **2010**, *297*, 187–191.
- ¹⁰³ Allen, M. P.; Tildesley, D. J.
Computer Simulation of Liquids, Oxford University Press, Oxford, 1987.
- ¹⁰⁴ Martínez-Veracoechea, F.; Müller, E. A.
Temperature-quench Molecular Dynamics Simulations for Fluid Phase Equilibria.
Mol. Sim., **2005**, *31*, 33–43.
- ¹⁰⁵ van der Spoel, D.; Lindahl, E.; Hess, B.; Groenhof, G.; Mark, A. E.; Berendsen, H. J. C.
GROMACS: Fast, Flexible, and Free.
J. Comput. Chem., **2005**, *26*, 1701–1718.
- ¹⁰⁶ Hoover, W. G.
Canonical Dynamics – Equilibrium Phase-Space Distributions.
Phys. Rev. A, **1985**, *31*, 1695–1697.
- ¹⁰⁷ Nosé, S.
A Unified Formulation of the Constant Temperature Molecular-Dynamics Methods.
J. Chem. Phys., **1984**, *81*, 511–519.
- ¹⁰⁸ Kirkwood, J. G.; Buff, F. P.
The Statistical Mechanical Theory of Surface Tension.
J. Chem. Phys., **1949**, *17*, 338–343.
- ¹⁰⁹ Gloor, G. J.; Jackson, G.; Blas, F. J.; de Miguel, E.
Test-area simulation method for the direct determination of the interfacial tension of systems with continuous or discontinuous potentials.
J. Chem. Phys., **2005**, *123*, 134703.
- ¹¹⁰ Eötvös, L.
Ueber den Zusammenhang der Oberflächenspannung der Flüssigkeiten mit ihrem Molecularvolumen".
Ann. Phys., **1886**, *27*, 448–459.
- ¹¹¹ Guggenheim, E. A.
The Principle of Corresponding States
J. Chem. Phys., **1945**, *13*, 253–261.
- ¹¹² Rebelo, L. P. N.; Canongia Lopes, J. N.; Esperança, J. M. S. S.; Filipe, E. J. M.
On the Critical Temperature, Normal Boiling Point, and Vapor Pressure of Ionic Liquids.
J. Phys. Chem. B, **2005**, *109*, 6040–6043.
- ¹¹³ Ambrose, D.; Tsonopoulos, C.
Vapor-Liquid Critical Properties of Elements and Compounds. 2. Normal Alkanes.
J. Chem. Eng. Data, **1995**, *40*, 531–546.
- ¹¹⁴ Marsh, K. N.; Abramson, A.; Ambrose, D.; Morton, D. W.; Nikitin, E.; Tsonopoulos, C.; Young, C. L.
Vapor-Liquid Critical Properties of Elements and Compounds. 10. Organic Compounds Containing Halogens.
J. Chem. Eng. Data, **2007**, *52*, 1509–1538.
- ¹¹⁵ Haszeldine, R. N.; Smith, F.
Organic Fluorides. Part VI. The Chemical and Physical Properties of Certain Fluorocarbons.
J. Chem. Soc., **1951**, 603–608.
- ¹¹⁶ McLure, I. A.; Whitfield, R.; Bowers, J.
Usual and Unusual Surface Tensions of Perfluorocarbon-Containing Binary Liquid Mixtures near a Critical Endpoint.
J. Colloid Interface Sci., **1998**, *203*, 31–40.
- ¹¹⁷ Adamson, A. W.; Gast, A. P.
Physical Chemistry of Surfaces (6th Ed.), Wiley-Interscience, New York (1997)
- ¹¹⁸ McLure, I. A.; Edmonds, B.; Lal, M.
Extremes in Surface Tension of Fluorocarbon+ Hydrocarbon Mixtures.
Nat. Phys. Sci., **1973**, *241*, 71.
- ¹¹⁹ Handa, T.; Mukerjee, P.

-
- Surface Tensions of Nonideal Mixtures of Fluorocarbons and Hydrocarbons and Their Interfacial Tensions against Water.
J. Phys. Chem., **1981**, *85*, 3916–3920.
- ¹²⁰ Bowers, J.; Clements, P. J.; McLure, I. A.; Burgess, A. N.
The Structure of the Liquid-Vapour Interface of n-Hexane + Perfluoro-n-Hexane along the Path of Critical Composition through the Critical End-Point by Neutron Reflectivity.
Mol. Phys., **1996**, *89*, 1825–1834.
- ¹²¹ Bowers, J.; McLure, I. A.; Whitfield, R.; Burgess, A. N.; Eaglesham, A.
Surface Composition Studies on (n -Hexane + Perfluoro- n -Hexane) by Specular Neutron Reflection.
Langmuir, **1997**, *13*, 2167–2170.
- ¹²² Bowers, J.; McLure, I. A.
A Regular Solution Theory Treatment of the Surface Tension of the Noncritical Liquid/Vapor Interface in Mixtures of a Dimethylsiloxane or an Alkane + a Perfluoroalkane near a Critical End Point.
Langmuir, **1996**, *12*, 3326–3333.
- ¹²³ MacLeod, D. B.
On a Relation Between Surface Tension and Density.
Trans. Faraday Soc., **1923**, *19*, 38–41.
- ¹²⁴ Sugden, S.
A Relation Between Surface Tension, Density and Chemical Composition.
J. Chem. Soc., **1924**, *125*, 1177–1189.
- ¹²⁵ Quayle, O. R.
The Parachors of Organic Compounds. An Interpretation and Catalogue.
Chem. Rev., **1953**, *53*, 439–589.
- ¹²⁶ Poling, B.E.; Prausnitz, J.M.; O’Connell, J.P.
The Properties of Gases and Liquids (5th Edition), McGraw-Hill, New York (2001)
- ¹²⁷ Sakka, T.; Ogata, Y. H.
Surface Tension of Fluoroalkanes in a Liquid Phase.
J. Fluor. Chem., **2005**, *126*, 371–375.
- ¹²⁸ Freire, M. G.; Carvalho, P. J.; Queimada, A. J.; Marrucho, I. M.; Coutinho, J. A. P.
Surface Tension of Liquid Fluorocompounds.
J. Chem. Eng. Data, **2006**, *51*, 1820–1824.
- ¹²⁹ Rohrback, G. H.; Cady, G. H.
Surface Tensions and Refractive Indices of the Perfluoropentanes.
J. Am. Chem. Soc., **1949**, *71*, 1938–1940.
- ¹³⁰ Fowler, R. D.; Hamilton Jr., J. M.; Kasper, J. S.; Weber, C. E.; Burford III, W. B.; Anderson, H. C. Physical and Chemical Properties of Pure Fluorocarbons.
Ind. Eng. Chem., **1947**, *39*, 375–378.
- ¹³¹ Oliver, G. D.; Blumkin, S.; Cunningham, C. W.
Some Physical Properties of Hexadecafluoroheptane.
J. Am. Chem. Soc., **1951**, *73*, 5722–5725.
- ¹³² Eppenga, R.; Frenkel, D.
Monte Carlo Study of the Isotropic and Nematic Phases of Infinitely Thin Hard Platelets.
Mol. Phys., **1984**, *52*, 1303–1334.
- ¹³³ Wu, L.; Malijevský, A.; Jackson, G.; Müller, E. A.; Avendaño, C.
Orientational Ordering and Phase Behaviour of Binary Mixtures of Hard Spheres and Hard Spherocylinders.
J. Chem. Phys., **2015**, *143*, 044906.